31. Miyazawa K, Nishimaki J, Katagiri T, et al. Thrombocytopenia induced by imatinib mesylate (Glivec) in patients with chronic myelogenous leukemia: is 400 mg daily of imatinib mesylate an optimal starting dose for Japanese patients? Int J Hematol. 2003;77:93–5. doi:10.1007/BF02982610.

32. Shah NP, Kantarjian HM, Kim DW, et al. Intermittent target inhibition with dasatinib 100 mg once daily preserves efficacy and improves tolerability in imatinib-resistant and intolerant chronic-phase chronic myeloid leukemia. J Clin Oncol. 2008;26:3204–12. doi:10.1200/JCO.2007.14.9260.

nature

Vol 460 | 13 August 2009 | doi:10.1038/nature08240

LETTERS

Gain-of-function of mutated *C-CBL* tumour suppressor in myeloid neoplasms

Masashi Sanada[1,5]*, Takahiro Suzuki[7]*, Lee-Yung Shih[8]*, Makoto Otsu[9], Motohiro Kato[1,2], Satoshi Yamazaki[6], Azusa Tamura[1], Hiroaki Honda[11], Mamiko Sakata-Yanagimoto[12], Keiki Kumano[3], Hideaki Oda[13], Tetsuya Yamagata[14], Junko Takita[1,2,3], Noriko Gotoh[10], Kumi Nakazaki[1,4], Norihiko Kawamata[15], Masafumi Onodera[16], Masaharu Nobuyoshi[7], Yasuhide Hayashi[17], Hiroshi Harada[18], Mineo Kurokawa[3,4], Shigeru Chiba[12], Hiraku Mori[18], Keiya Ozawa[7], Mitsuhiro Omine[18], Hisamaru Hirai[3,4], Hiromitsu Nakauchi[6,9], H. Phillip Koeffler[15] & Seishi Ogawa[1,5]

Acquired uniparental disomy (aUPD) is a common feature of cancer genomes, leading to loss of heterozygosity. aUPD is associated not only with loss-of-function mutations of tumour suppressor genes[1], but also with gain-of-function mutations of proto-oncogenes[2]. Here we show unique gain-of-function mutations of the *C-CBL* (also known as *CBL*) tumour suppressor that are tightly associated with aUPD of the 11q arm in myeloid neoplasms showing myeloproliferative features. The *C-CBL* proto-oncogene, a cellular homologue of *v-Cbl*, encodes an E3 ubiquitin ligase and negatively regulates signal transduction of tyrosine kinases[3–6]. Homozygous *C-CBL* mutations were found in most 11q-aUPD-positive myeloid malignancies. Although the *C-CBL* mutations were oncogenic in NIH3T3 cells, c-Cbl was shown to functionally and genetically act as a tumour suppressor. C-CBL mutants did not have E3 ubiquitin ligase activity, but inhibited that of wild-type C-CBL and CBL-B (also known as CBLB), leading to prolonged activation of tyrosine kinases after cytokine stimulation. *c-Cbl*$^{-/-}$ haematopoietic stem/progenitor cells (HSPCs) showed enhanced sensitivity to a variety of cytokines compared to *c-Cbl*$^{+/+}$ HSPCs, and transduction of *C-CBL* mutants into *c-Cbl*$^{-/-}$ HSPCs further augmented their sensitivities to a broader spectrum of cytokines, including stem-cell factor (SCF, also known as KITLG), thrombopoietin (TPO, also known as THPO), IL3 and FLT3 ligand (FLT3LG), indicating the presence of a gain-of-function that could not be attributed to a simple loss-of-function. The gain-of-function effects of C-CBL mutants on cytokine sensitivity of HSPCs largely disappeared in a *c-Cbl*$^{+/+}$ background or by co-transduction of wild-type *C-CBL*, which suggests the pathogenic importance of loss of wild-type *C-CBL* alleles found in most cases of *C-CBL*-mutated myeloid neoplasms. Our findings provide a new insight into a role of gain-of-function mutations of a tumour suppressor associated with aUPD in the pathogenesis of some myeloid cancer subsets.

Myelodysplastic syndromes (MDS) are heterogeneous groups of blood cancers originating from haematopoietic precursors. They are characterized by deregulated haematopoiesis showing a high propensity to acute myeloid leukaemia (AML)[7]. Some MDS cases have overlapping clinico-pathological features with myeloproliferative disorders, and are now classified into myelodysplasia/myeloproliferative neoplasms (MDS/MPN) by the World Health Organization (WHO) classification[8]. To obtain a comprehensive profile of allelic imbalances in these myeloid neoplasms, we performed allele-specific copy number analyses of bone marrow samples obtained from 222 patients with MDS, MDS/MPN, or other related myeloid neoplasms (Supplementary Tables 1 and 2) using high-density single nucleotide polymorphism (SNP) arrays combined with CNAG/AsCNAR software[9,10].

Genomic profiles of MDS and MDS/MPN showed characteristic unbalanced genetic changes, as reported in previous cytogenetic studies[11] (Supplementary Fig. 1a); however, they were detected more sensitively by SNP array analyses (Supplementary Table 3). aUPD was detected in 70 samples (31.5%) on the basis of the allele-specific copy number analyses, which substantially exceeded the detection rate obtained using a SNP call-based detection algorithm (20.7%) (Supplementary Figs 2 and 4, and Supplementary Tables 4 and 5). Long stretches of homozygous SNP calls caused by shared identical-by-descent alleles in parents were empirically predicted and excluded (Supplementary Fig. 3). aUPDs were more common in MDS/MPN than in MDS. They preferentially affected several chromosomal arms (1p, 1q, 4q, 7q, 11p, 11q, 14q, 17p and 21q) in distinct subsets of patients, and frequently associated with mutated oncogenes and tumour suppressor genes (Supplementary Figs 1b and 5). Among these, the most common aUPDs were those involving 11q ($n = 17$), which defined a unique subset of myeloid neoplasms that were clinically characterized by frequent diagnosis of chronic myelomonocytic leukaemia (CMML) with normal karyotypes (13 cases) (Fig. 1a and Supplementary Table 6). We identified a minimum overlapping aUPD segment of approximately 1.4 megabases (Mb) in 11q, which contained a mutated *C-CBL* proto-oncogene (Fig. 1b).

[1]Cancer Genomics Project, [2]Department of Pediatrics, [3]Cell Therapy and Transplantation Medicine, and [4]Hematology and Oncology, Graduate School of Medicine, The University of Tokyo, 7-3-1 Hongo, Bunkyo-ku, Tokyo 113-8655, Japan. [5]Core Research for Evolutional Science and Technology, [6]Exploratory Research for Advanced Technology, Japan Science and Technology Agency, 4-1-8 Honcho, Kawaguchi-shi, Saitama 332-0012, Japan. [7]Division of Hematology, Department of Medicine, Jichi Medical University, 3311-1 Yakushiji, Shimotsuke-shi, Tochigi 329-0498, Japan. [8]Division of Hematology-Oncology, Department of Internal Medicine, Chang Gung Memorial Hospital, Chang Gung University, 199 Tung Hwa North Road, Taipei 105, Taiwan. [9]Division of Stem Cell Therapy, Center for Stem Cell and Regenerative Medicine, [10]Division of Systems Biomedical Technology, Institute of Medical Science, The University of Tokyo, 4-6-1 Shirokanedai, Minato-ku, Tokyo 108-8639, Japan. [11]Department of Developmental Biology, Research Institute of Radiation Biology and Medicine, Hiroshima University, 1-2-3 Kasumi, Minami-ku, Hiroshima 734-8553, Japan. [12]Department of Clinical and Experimental Hematology, Institute of Clinical Medicine, University of Tsukuba, 1-1-1 Tennodai, Tukuba-shi, Ibaraki, 305-8571, Japan. [13]Department of Pathology, Tokyo Women's Medical University, 8-1 Kawada-cho, Shinjuku-ku, Tokyo 162-8666, Japan. [14]Department of Hematology, Dokkyo University School of Medicine, 800 Kitabayashi, Mibu, Tochigi 321-0293, Japan. [15]Hematology/Oncology, Cedars-Sinai Medical Center, 8700 Beverly Boulevard, Los Angeles, California 90048, USA. [16]Department of Genetics, National Research Institute for Child Health and Development, 2-10-1 Okura, Setagaya-ku, Tokyo, 157-8535, Japan. [17]Gunma Children's Medical Center, 779 Shimohakoda, Hokkitsu-machi, Shibukawa-shi, Gunma 377-8577, Japan. [18]Division of Hematology, Internal Medicine, Showa University Fujigaoka Hospital, 1-30 Fujigaoka, Aoba-ku, Yokohama, Kanagawa 227-8501, Japan.
*These authors contributed equally to this work.

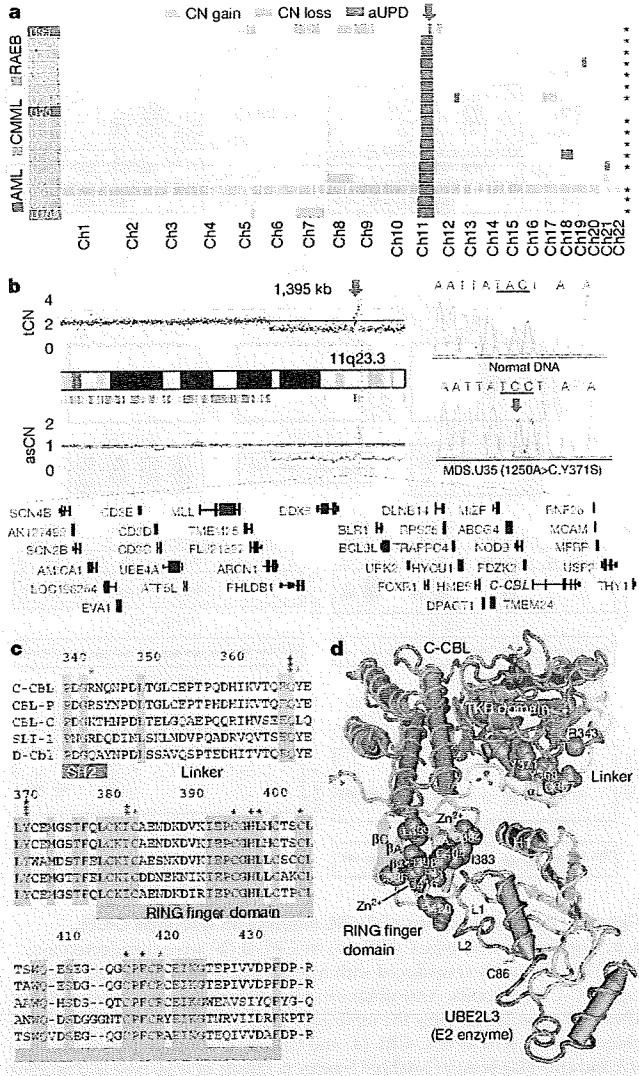

Figure 1 | Common UPD on the 11q arm and *C-CBL* mutations in myeloid neoplasms. **a**, Copy number profiles of 17 cases with myeloid neoplasms showing 11qUPD. Regions of copy number (CN) gains, losses and aUPD are depicted in different colours. Histologies are shown by coloured boxes. Asterisks denote *C-CBL*-mutated cases. Ch, chromosome; RAEB, refractory anaemia with excess blasts. **b**, CNAG output for MDS.U35. Total copy number (tCN) and allele-specific copy number (asCN) plots show a focal copy number gain spanning a 1.4-Mb segment within 3 Mb of an 11q-aUPD region (left), which contained mutated *C-CBL* in MDS.U35 (right). **c**, Alignments of amino acid sequences for human CBL family proteins and their homologues in *Caenorhabditis elegans* (SLI-1) and *Drosophila* (D-Cbl). Amino acid numbering is on the basis of human *C-CBL*. Conserved amino acids are highlighted. Positions of mutated amino acids are indicated by asterisks. Heterozygous mutations are shown in red. **d**, Mutated amino acid positions in the three-dimensional structure of a human C-CBL–UBE2L3 complex. TKB, tyrosine kinase binding domain.

C-CBL is the cellular homologue of the *v-Cbl* transforming gene of the Cas NS-1 murine leukaemia virus[5,12]. It was recently found to be mutated in human AML cases[13–15]. Together with its close homologue, CBL-B, C-CBL is thought to be involved in the negative modulation of tyrosine kinase signalling, primarily through their E3 ubiquitin ligase activity that is responsible for the downregulation of activated tyrosine kinases[2–5]. By sequencing all *C-CBL* exons in all 222 samples, we found *C-CBL* mutations in 15 of the 17 cases with 11q-aUPD, whereas only 3 out of 205 cases without 11q-aUPD had *C-CBL* mutations, showing a strong association of *C-CBL* mutations with 11q-aUPD ($P = 1.46 \times 10^{-18}$) (Supplementary Fig. 6 and Supplementary Tables 6 and 7), as also indicated in a recent report[16]. Thus, *C-CBL* was thought to be the major, if not the only, target of 11q-aUPD in myeloid neoplasms. Two different *C-CBL* mutations co-existed in three cases (Supplementary Fig. 6b). Somatic origins of the mutations were confirmed in three evaluable cases (Supplementary Fig. 6c).

In most cases, *C-CBL* mutations were missense, involving the evolutionarily conserved amino acids within the linker-RING finger domain that is central to the E3 ubiquitin ligase activity[17] (Fig. 1c). Another case with a predominant Cys384Tyr mutation also contained a nonsense mutation (Arg343X) in a minor subclone, which resulted in a v-Cbl-like truncated protein (Supplementary Fig. 6b). In the remaining two cases, mutations led to amino acid deletions (Δ369−371 and Δ368−382) involving the highly conserved α-helix (αL) of the linker domain and the first loop of the RING finger. According to the published crystal structure of *C-CBL*[17], most of the mutated or deleted amino acids were positioned on the interface for the binding to the E2 enzyme (Fig. 1d), making contact with either the tyrosine kinase binding domain (Tyr 368 and Tyr 371) or E2 ubiquitin-conjugating enzymes (Ile 383, Cys 404 and Phe 418). Especially, all seven linker-domain mutations selectively involved just three amino acids (Gln 367, Tyr 368 and Tyr 371) within the conserved αL helix (Fig. 1d). Mutations were clearly homozygous in nine cases, and the apparently heterozygous chromatograms in the other six cases could also be compatible with homozygous mutations affecting the aUPD-positive tumour clones, given the presence of substantial normal cell components within these samples. Mutations in the remaining three cases were considered to be heterozygous. About half of the *C-CBL*-mutated cases carried coexisting mutations of *RUNX1* (four cases), *TP53* (one case), *FLT3* internal tandem duplication (1 case) or *JAK2* (3 cases). *NRAS* and *KRAS* mutations were prevalent among CMML (15.1%) but occurred within discrete clusters from *C-CBL*-mutated cases (Supplementary Tables 2 and 6 and Supplementary Fig. 5). The mutation status of *C-CBL* did not substantially affect the clinical outcome (Supplementary Fig. 7).

All tested *C-CBL* mutants induced clear oncogenic phenotypes in NIH3T3 fibroblasts, as demonstrated by enhanced colony formation in soft agar and tumour generation in nude mice (Supplementary Fig. 8). Transformed NIH3T3 cells showed PI3 kinase-dependent activation of Akt and the transformed phenotype was reverted by treatment with the PI3 kinase inhibitor Ly294002 (Supplementary Fig. 9). When introduced into Lin^- $Sca1^+$ c-Kit^+ (LSK) HSPCs, C-CBL mutants (C-CBL(Gln367Pro) and C-CBL(Tyr371Ser)), as well as a mouse lymphoma-derived oncogenic mutant (C-CBL(70Z)), significantly promoted the replating capacity of these progenitors (Fig. 2a). Because c-Cbl negatively modulates tyrosine kinase signalling, and all *C-CBL* mutations, including those previously reported[13–16], affected the critical domains for its enzymatic activity involved in this modulation, C-CBL was postulated to have a tumour suppressor function; loss-of-function could be a mechanism for the oncogenicity of these C-CBL mutants[3–5]. To assess this possibility and to clarify further the role of *C-CBL* mutations in the pathogenesis of myeloid neoplasms, we generated *c-*$Cbl^{-/-}$ mice and examined their haematological phenotypes (Supplementary Fig. 10).

In agreement with previous reports[18–20], *c-*$Cbl^{-/-}$ mice exhibited splenomegaly and an augmented haematopoietic progenitor pool, as was evident from the increased colony formation of bone marrow cells in methylcellulose culture and higher numbers of LSK and CD34-negative LSK cells in bone marrow and/or spleen compared to their wild-type littermates (Fig. 2b–d and Supplementary Fig. 11). Furthermore, when introduced into a *BCR-ABL* transgenic background[21], the *c-*$Cbl^{-/-}$ allele accelerated blastic crisis depending on the allele dosage (Fig. 2e, f). These observations supported the notion that wild-type *C-CBL* has tumour suppressor functions, whereas 'mutant' *C-CBL* acts as an oncogene; *C-CBL* can therefore be both a proto-oncogene and a tumour suppressor gene.

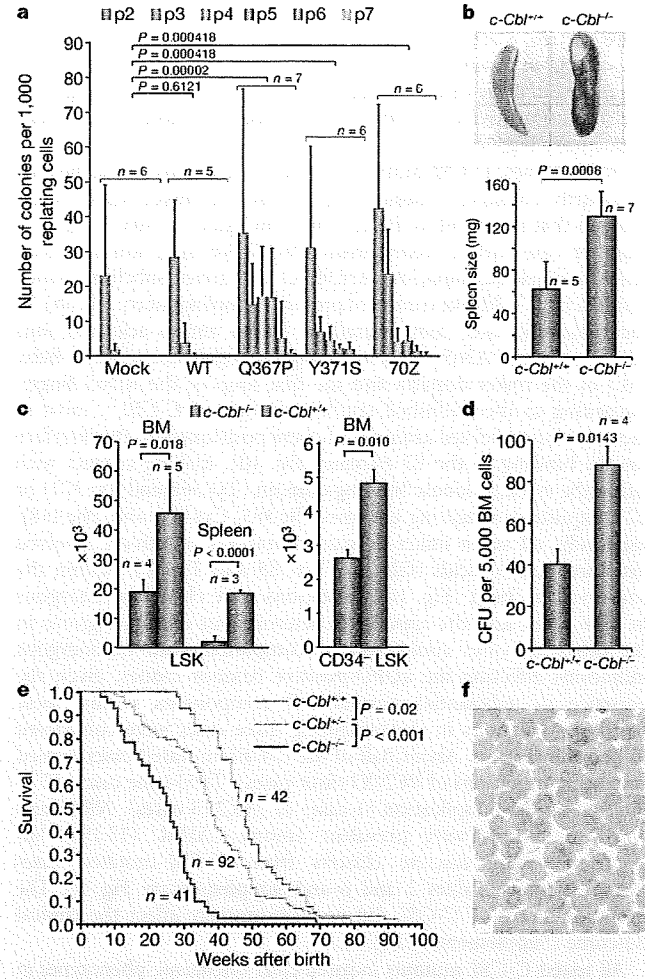

Figure 2 | Tumour-suppressor functions of wild-type C-CBL. **a**, Prolonged replating capacity of LSK cells transduced with mutant *C-CBL* (*C-CBL*(Gln367Pro) and *C-CBL*(Tyr371Ser)), compared to mock- or wild-type *C-CBL*-transduced cells. Replating capacity in methylcellulose culture is shown as mean colony number (and s.d.) per 1,000 replating cells at indicated times of replating. p, passage. **b**, Increased spleen mass in *c-Cbl*$^{-/-}$ mice compared to *c-Cbl*$^{+/-}$ mice (mean spleen weight and s.d.). **c**, Mean number of total LSK (left) and CD34-negative LSK (right) cells (plus s.d.) in bone marrow (BM) and/or spleen in *c-Cbl*$^{+/+}$ (blue columns) and *c-Cbl*$^{-/-}$ mice (red columns). Bone marrow cells from bilateral tibias and femurs were counted for each mouse. **d**, Augmented colony-forming potential of bone marrow cells from *c-Cbl*$^{-/-}$ mice (mean colony number and s.d. per 5,000 bone marrow cells). CFU, colony-forming units. **e**, Kaplan–Meier survival curves of *c-Cbl*$^{+/+}$, *c-Cbl*$^{+/-}$ and *c-Cbl*$^{-/-}$ mice carrying a *BCR-ABL* transgene, showing acceleration of blastic crisis in *c-Cbl*$^{+/-}$ and *c-Cbl*$^{-/-}$ mice. **f**, Wright–Giemsa staining of an enlarged lymph node in a *Bcr-Abl*$^{+}$ *c-Cbl*$^{-/-}$ mouse during blastic crisis shows massive infiltrates of immature leukaemic blasts. Original magnification, ×600.

Mouse LSK HSPCs expressed two Cbl family member proteins: wild-type c-Cbl and Cbl-b (Supplementary Fig. 12)[22]. When transduced into NIH3T3 cells stably expressing human epidermal growth factor receptor (EGFR), both Cbl proteins enhanced ubiquitination of EGFR after EGF stimulation, which was suppressed by coexpression of the C-CBL mutants (Fig. 3a, b). In haematopoietic cells, overexpression of wild-type C-CBL enhanced ligand-induced ubiquitination of a variety of tyrosine kinases, including c-KIT, FLT3 and JAK2. In contrast, C-CBL mutants not only showed compromised enzymatic activity, but also inhibited the ubiquitinating activities in these haematopoietic cells (Fig. 3c), leading to prolonged tyrosine kinase activation after ligand stimulation (Fig. 3d).

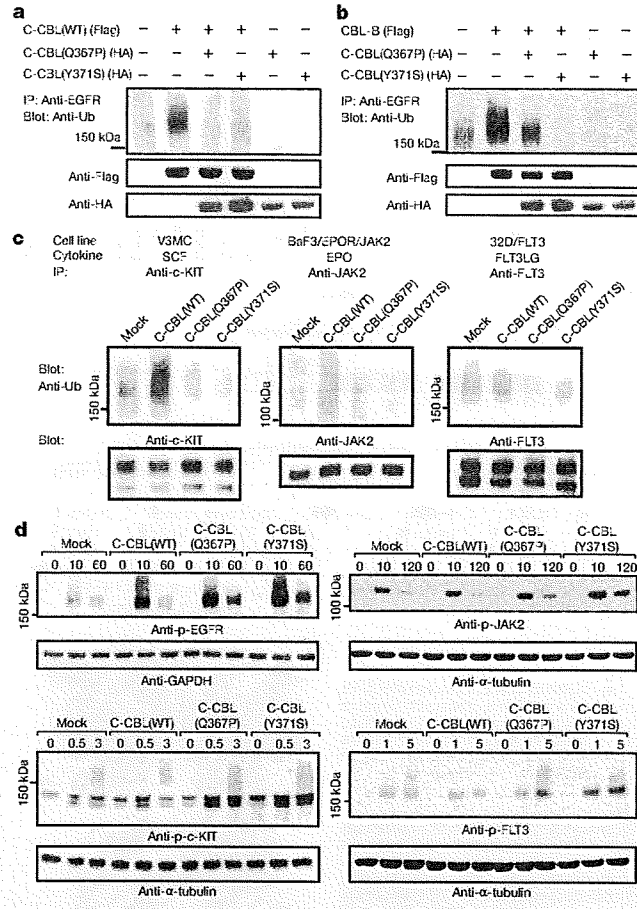

Figure 3 | Inhibitory actions of C-CBL mutants on wild-type C-CBL. **a**, **b**, Flag-tagged wild-type C-CBL (**a**) or CBL-B (**b**) were transfected into NIH3T3 cells stably transduced with human EGFR plus indicated HA-tagged C-CBL mutants. Anti-ubiquitin blots of immunoprecipitated EGFR after EGF stimulation show the inhibitory actions of the C-CBL mutants on ubiquitinating activity of C-CBL (**a**) and CBL-B (**b**). Bottom panels are anti-HA and anti-Flag blots of total cell lysates. **c**, Effects of wild-type and mutant C-CBL on cytokine-induced ubiquitination of c-KIT, JAK2 and FLT3 in haematopoietic cells V3MC, BaF3 co-transduced with human erythropoietin receptor (EPOR) and JAK2 (BaF3/EPOR/JAK2), and FLT3-transduced 32D (32D/FLT3), respectively. Each cell line was further transduced with indicated C-CBL mutants, and ubiquitination of immunoprecipitated kinases was detected by anti-ubiquitin blots at 1 min after stimulation with SCF, EPO and FLT3LG. Anti-kinase blots of the precipitated kinases are shown below each panel. **d**, Kinase phosphorylation was examined at indicated time points (shown in minutes) after ligand stimulation using immunoblot analyses of total cell lysates using antibodies to phosphorylated (p-) EGFR, c-KIT, JAK2 and FLT3 in which anti-α-tubulin or anti-GAPDH blots are provided as a control.

Because tyrosine kinase signalling is central to cytokine responses in haematopoietic cells and its deregulation is a common feature of myeloproliferative disorders[23], we next examined the effects of *C-CBL* mutations (*C-CBL*(Gln367Pro) and *C-CBL*(Tyr371Ser)) and the loss of wild-type *C-CBL* alleles on the responses of LSK HSPCs to various cytokines. In serum-free conditions, *c-Cbl*$^{-/-}$ LSK cells showed a modestly enhanced proliferative response to a variety of cytokines, including SCF, IL3 and TPO, compared to *c-Cbl*$^{+/+}$ cells (mock columns in Fig. 4a). However, the enhanced response in *c-Cbl*$^{-/-}$ cells was markedly augmented and extended to a broader spectrum of cytokines, including FLT3 ligand by the transduction of *C-CBL* mutants. Of note, the effect of *C-CBL* mutant transduction was not remarkable in *c-Cbl*$^{-/+}$ LSK cells except for the response to SCF, which was clearly enhanced by *C-CBL* mutants

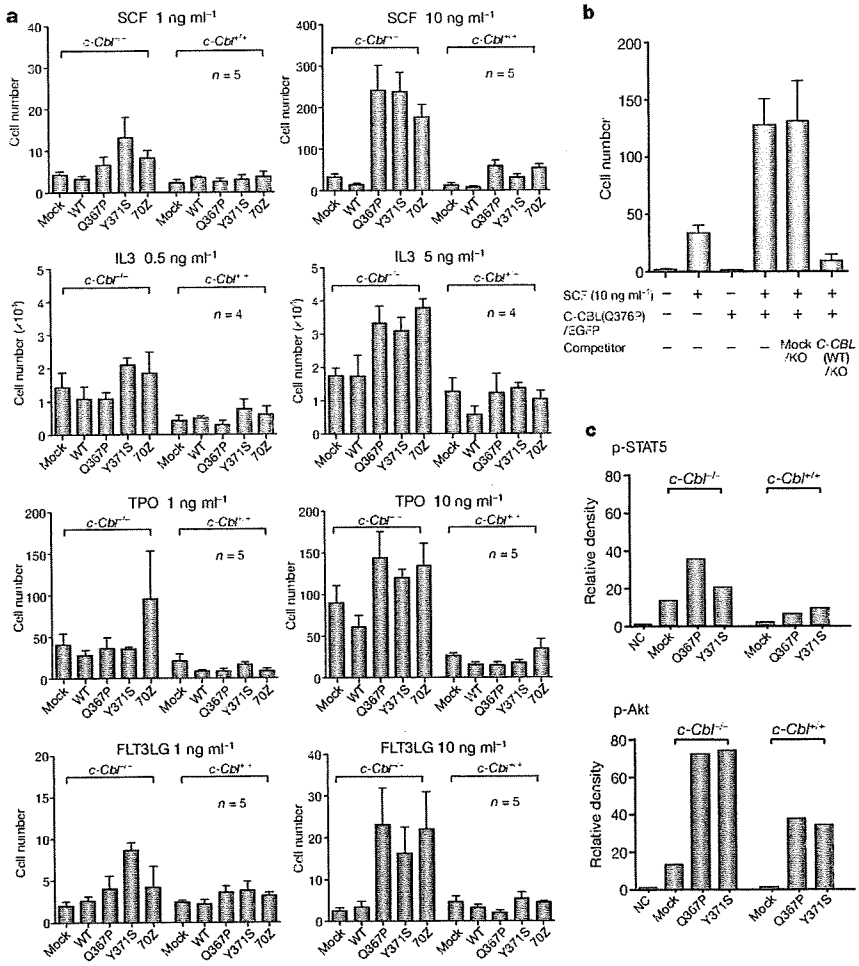

Figure 4 | Gain-of-function of mutant C-CBL augmented by loss of wild-type C-CBL. **a**, *c-Cbl*$^{+/+}$ and *c-Cbl*$^{-/-}$ LSK cells were transfected with various *C-CBL* internal ribosome entry site (IRES)/green fluorescent protein (GFP) constructs, and 50 GFP-positive cells were sorted for serum-free culture containing indicated concentrations of SCF, IL3, TPO and FLT3LG. Mean cell numbers (plus s.e.m.) on day 5 are plotted. **b**, *c-Cbl*$^{-/-}$ LSK cells were co-transduced with C-CBL(Gln367Pro)-IRES-EGFP (C-CBL(Q367P)/EGFP) and mock-IRES-Kusabira-Orange (mock/KO) or wild-type *C-CBL*-IRES-Kusabira-Orange (*C-CBL*(WT)/KO), and 50 GFP/KO double-positive cells were sorted into each well for cell proliferation assays in serum-free culture containing 10 ng ml^{-1} SCF. Mean cell numbers on day 5 (plus s.e.m., $n = 5$) are plotted. **c**, Ten thousand *c-Cbl*$^{+/+}$ and *c-Cbl*$^{-/-}$ LSK cells transduced with various C-CBL constructs were stimulated with 10 ng ml^{-1} SCF and 10 ng ml^{-1} TPO for 15 min. Total cell lysates were analysed by immunoblotting, using antibodies to STAT5, Akt and their phosphorylated forms. The intensities of phosphorylated proteins relative to total STAT5 (top panel) and Akt (bottom panel) are plotted. NC indicates the mean background signal obtained with nonspecific IgG.

even with a *c-Cbl*$^{+/+}$ background (Fig. 4a and Supplementary Fig. 13). To clarify further the effect of wild-type C-CBL on C-CBL mutants, both wild-type C-CBL and C-CBL mutants were co-transduced into *c-Cbl*$^{-/-}$ LSK cells, and their effects on the response to SCF were examined. As shown in Fig. 4b, the hyperproliferative response induced by C-CBL mutants was almost completely abolished by the co-transduction of wild-type C-CBL, suggesting the pathogenic importance of loss of wild-type *C-CBL* alleles found in most *C-CBL*-mutated cases. LSK cells transduced with C-CBL mutants also showed enhanced activation of the STAT5 and Akt pathways on cytokine stimulation (SCF and TPO), which was more pronounced in *c-Cbl*$^{-/-}$ than *c-Cbl*$^{+/+}$ LSK cells (Fig. 4c and Supplementary Fig. 14).

The modest enhancement of sensitivity to cytokines found in *c-Cbl*$^{-/-}$ LSK cells was a consequence of loss of C-CBL functions. In contrast, the hypersensitive response of mutant-transduced *c-Cbl*$^{-/-}$ LSK cells to a broad spectrum of cytokines represents gain-of-function of the mutants that could not be ascribed to a simple loss of C-CBL functions, which was also predicted from the strong association of *C-CBL* mutations with 11q-aUPD by analogy to the gain-of-function *JAK2* mutations associated with 9p-aUPD in polycythemia vera[2]. The gain-of-function of C-CBL mutants became more evident under a *c-Cbl*$^{-/-}$ background. The hypersensitive response to cytokines induced by mutant C-CBL under the *c-Cbl*$^{-/-}$ background was largely offset by the presence of the wild-type *c-Cbl* allele or by the transduction of the wild-type C-CBL gene, suggesting that the gain-of-function could be closely related to loss of C-CBL-like functions, probably by inhibition of Cbl-b. Supporting this view is a previous report that *c-Cbl/Cbl-b* double knockout T cells showed more profound impairments in the downregulation of the T-cell receptor (TCR), more sustained TCR signalling, and more vigorous proliferation, than *c-Cbl* or *Cbl-b* single knockout T cells after anti-CD3 (also known as CD3e) stimulation[24]. This is analogous to the gain-of-function found in some TP53 mutants, which has been explained by functional inhibition of two TP53 homologues, TP73 and TP63 (refs 25, 26). Of note, TP53 was also originally isolated as an oncogene through its mutated forms[27]. The Cbl-b inhibition-based gain-of-function model could be tested directly by comparing the behaviour of *c-Cbl/Cbl-b* double knockout LSK cells with that of LSK cells carrying homozygously knocked-in mutant *C-CBL* alleles. On the other hand, there remains a possibility that the gain-of-function could be mediated by a mechanism other than the simple inhibition of the homologue, because C-CBL mutants retained several motifs

that interacted with numerous signal-transducing molecules. Furthermore, considering the ubiquitous expression of CBL proteins, it would be of interest to explore the possible involvement of mutations in all *CBL* family members in other human cancers.

METHODS SUMMARY

Genomic DNA from 222 bone marrow samples with myeloid neoplasms were analysed using GeneChip SNP-genotyping microarrays (Affymetrix GeneChip) as described[28]. Allelic imbalances were detected from the allele-specific copy numbers calculated using CNAG/AsCNAR software (http://www.genome.umin.jp)[9,10]. *C-CBL* mutations were examined by sequencing PCR-amplified genomic DNA. For functional assays, haemagglutinin (HA)- or Flag-tagged complementary DNAs of wild-type and mutant *C-CBL* were generated by *in vitro* mutagenesis, constructed into a MSCV-based retroviral vector, pGCDNsamIRESGFP or pGCDNsamIRESKO, and used for retrovirus-mediated gene transfer. For the evaluation of oncogenicity of C-CBL mutants, NIH3T3 cells were transfected with various *C-CBL* constructs and used for colony assays in soft agar and tumour formation assays in nude mice. *c-Cbl*-deficient mice were generated using a conventional strategy of gene-targeting and crossed with *BCR-ABL* transgenic mice to evaluate the effect of the *c-Cbl*$^{-}$ allele on the acceleration of blastic crisis. LSK cells sorted from *c-Cbl*$^{+/+}$ and *c-Cbl*$^{-/-}$ mice were transduced with various *C-CBL* constructs. Their responses to cytokines were evaluated by cell proliferation assays, followed by immunoblot analyses of c-KIT, FLT3 and JAK2, as well as their downstream signalling molecules. The effects of C-CBL mutant expression on the ubiquitination of EGFR, c-KIT, FLT3 and JAK2 were examined by transducing C-CBL mutants into relevant cells, followed by anti-ubiquitin blots of the immunoprecipitated kinases after ligand stimulation. Functional competition of C-CBL mutants with wild-type C-CBL was assessed by cell proliferation assays of LSK cells co-transduced with both wild-type and mutant C-CBL genes. This study was approved by the ethics boards of the University of Tokyo, Chang Gung Memorial Hospital and Showa University. Antibodies and primers used in this study are listed in Supplementary Tables 8 and 9.

Full Methods and any associated references are available in the online version of the paper at www.nature.com/nature.

Received 9 October 2008; accepted 30 June 2009.
Published online 20 July 2009.

1. Knudson, A. G. Two genetic hits (more or less) to cancer. *Nature Rev. Cancer* 1, 157–162 (2001).
2. James, C. *et al.* A unique clonal JAK2 mutation leading to constitutive signalling causes polycythaemia vera. *Nature* 434, 1144–1148 (2005).
3. Ryan, P. E. *et al.* Regulating the regulator: negative regulation of Cbl ubiquitin ligases. *Trends Biochem. Sci.* 31, 79–88 (2006).
4. Schmidt, M. H. & Dikic, I. The Cbl interactome and its functions. *Nature Rev. Mol. Cell Biol.* 6, 907–918 (2005).
5. Thien, C. B. & Langdon, W. Y. Cbl: many adaptations to regulate protein tyrosine kinases. *Nature Rev. Mol. Cell Biol.* 2, 294–307 (2001).
6. Thien, C. B. & Langdon, W. Y. c-Cbl and Cbl-b ubiquitin ligases: substrate diversity and the negative regulation of signalling responses. *Biochem. J.* 391, 153–166 (2005).
7. Corey, S. J. *et al.* Myelodysplastic syndromes: the complexity of stem-cell diseases. *Nature Rev. Cancer* 7, 118–129 (2007).
8. Jaffe, E., Harris, N., Stein, H. & Vardiman J. *World Health Organization Classification of Tumours: Pathology and Genetics of Tumours of Haematopoietic and Lymphoid Tissues* 62–73 (IARC Press, 2002).
9. Nannya, Y. *et al.* A robust algorithm for copy number detection using high-density oligonucleotide single nucleotide polymorphism genotyping arrays. *Cancer Res.* 65, 6071–6079 (2005).
10. Yamamoto, G. *et al.* Highly sensitive method for genomewide detection of allelic composition in nonpaired, primary tumor specimens by use of affymetrix single-nucleotide-polymorphism genotyping microarrays. *Am. J. Hum. Genet.* 81, 114–126 (2007).
11. Haase, D. Cytogenetic features in myelodysplastic syndromes. *Ann. Hematol.* 87, 515–526 (2008).
12. Langdon, W. Y. *et al.* v-cbl, an oncogene from a dual-recombinant murine retrovirus that induces early B-lineage lymphomas. *Proc. Natl Acad. Sci. USA* 86, 1168–1172 (1989).
13. Abbas, S. *et al.* Exon 8 splice site mutations in the gene encoding the E3-ligase C3L are associated with core binding factor acute myeloid leukemias. *Haematologica* 93, 1595–1597 (2008).
14. Caligiuri, M. A. *et al.* Novel c-CBL and CBL-b ubiquitin ligase mutations in human acute myeloid leukemia. *Blood* 110, 1022–1024 (2007).
15. Sargin, B. *et al.* Flt3-dependent transformation by inactivating c-Cbl mutations in AML. *Blood* 110, 1004–1012 (2007).
16. Dunbar, A. J. *et al.* 250K single nucleotide polymorphism array karyotyping identifies acquired uniparental disomy and homozygous mutations, including novel missense substitutions of c-Cbl, in myeloid malignancies. *Cancer Res.* 68, 10349–10357 (2008).
17. Zheng, N. *et al.* Structure of a c-Cbl-UbcH7 complex: RING domain function in ubiquitin-protein ligases. *Cell* 102, 533–539 (2000).
18. Murphy, M. A. *et al.* Tissue hyperplasia and enhanced T-cell signalling via ZAP-70 in c-Cbl-deficient mice. *Mol. Cell. Biol.* 18, 4872–4882 (1998).
19. Naramura, M. *et al.* Altered thymic positive selection and intracellular signals in Cbl-deficient mice. *Proc. Natl Acad. Sci. USA* 95, 15547–15552 (1998).
20. Rathinam, C. *et al.* The E3 ubiquitin ligase c-Cbl restricts development and functions of hematopoietic stem cells. *Genes Dev.* 22, 992–997 (2008).
21. Honda, H. *et al.* Acquired loss of p53 induces blastic transformation in p210(bcr/abl)-expressing hematopoietic cells: a transgenic study for blast crisis of human CML. *Blood* 95, 1144–1150 (2000).
22. Zeng, S. *et al.* Regulation of stem cell factor receptor signaling by Cbl family proteins (Cbl-b/c-Cbl). *Blood* 105, 226–232 (2005).
23. Kaushansky, K. Hematopoietic growth factors, signaling and the chronic myeloproliferative disorders. *Cytokine Growth Factor Rev.* 17, 423–430 (2006).
24. Naramura, M. *et al.* c-Cbl and Cbl-b regulate T cell responsiveness by promoting ligand-induced TCR down-modulation. *Nature Immunol.* 3, 1192–1199 (2002).
25. Dittmer, D. *et al.* Gain of function mutations in p53. *Nature Genet.* 4, 42–46 (1993).
26. Lang, G. A. *et al.* Gain of function of a p53 hot spot mutation in a mouse model of Li-Fraumeni syndrome. *Cell* 119, 861–872 (2004).
27. Finlay, C. A., Hinds, P. W. & Levine, A. J. The p53 proto-oncogene can act as a suppressor of transformation. *Cell* 57, 1083–1093 (1989).
28. Chen, Y. *et al.* Oncogenic mutations of ALK kinase in neuroblastoma. *Nature* 455, 971–974 (2008).

Supplementary Information is linked to the online version of the paper at www.nature.com/nature.

Acknowledgements This work was supported by the Core Research for Evolutional Science and Technology, Japan Science and Technology Agency, a Grant-in-Aid from the Ministry of Health, Labor and Welfare of Japan and from the Ministry of Education, Culture, Sports, Science and Technology, and a grant from National Health Research Institute, Taiwan, NHRI-EX96-9434SI, and NIH-2R01CA026038-30. We thank W. Y. Langdon for providing a human *C-CBL* cDNA. A mast-cell cell line expressing c-KIT V3MC was a gift from M. F. Gurish. We also thank Y. Ogino and K. Fujita for their technical assistance.

Author Contributions M.S. and M.Kato performed microarray experiments and subsequent data analyses. T.S., T.Y., H.Honda and H.Hirai generated and analysed *c-Cbl*-null mice. M.S., M.Otsu, S.Y., M.N., K.K., N.G., M.Onodera, M.S.-Y. and H.N. conducted functional assays of C-CBL mutants. L.-Y.S., M.S., M.Kato, K.N., J.T. and A.T. performed mutation analysis. H.O. performed pathological analysis of *c-Cbl*-null mice. L.-Y.S., N.K., H.Harada, M.Kurokawa, S.C., H.M., H.P.K. and M.Omine prepared MDS specimens. M.S., M.Otsu, Y.H., K.O., H.M., H.N., L.-Y.S., H.P.K. and S.O. designed the overall study, and S.O. wrote the manuscript. All authors discussed the results and commented on the manuscript.

Author Information Full copy number data for the 222 samples are accessible from the Gene Expression Omnibus public database (http://ncbi.nlm.nih.gov/geo/) with the accession number GSE15187. Reprints and permissions information is available at www.nature.com/reprints. Correspondence and requests for materials should be addressed to S.O. (sogawa-tky@umin.ac.jp) or L.-Y.S. (s.y7012@adm.cgmh.org.tw).

METHODS

Genome-wide analysis of allelic imbalances in primary myeloid neoplasms. Bone marrow specimens were obtained from 222 patients diagnosed with myeloid neoplasms according to the WHO classification (Supplementary Tables 1 and 2). High molecular weight genomic DNA was extracted and used for microarray analysis using Affymetrix GeneChip 50K XbaI, HindIII or 250K NspI, according to the manufacturer's instructions. Genome-wide detection of allelic imbalances was performed using CNAG/AsCNAR software (http://www.genome.umin.jp)[9,10].

Mutation analysis. Mutation analysis was performed by direct sequencing of PCR-amplified coding exons of the relevant genes, using an ABI PRISM 3100 genetic analyser (Applied Biosystems). The target genes, exons and PCR primers are listed in Supplementary Table 8. Tandem duplication of the *FLT3* gene was examined by genomic PCR and sequencing.

Preparation of high-titre vesicular stomatitis virus glycoprotein (VSV-G)-pseudotyped retroviral particles. HA-tagged human *C-CBL* cDNA was a gift from W. Y. Langdon. Nine mutant cDNAs of *C-CBL*, including eight from patients' specimens and a 70Z mutant corresponding to a mutant isolated from mouse lymphoma[29], were generated on the basis of this construct, using a QuickChange site-directed mutagenesis kit (Stratagene). These were then constructed into the retrovirus vectors pGCDNsamIRESGFP and pGCDNsamIRESKO[30–32]. Vector plasmids were co-transfected with a VSV-G cDNA into 293GP cells (provided by R. C. Mulligan) to obtain retrovirus-containing supernatant, which was then transduced into 293GPG cells to establish stable cell lines capable of producing VSV-G-pseudotyped retroviral particles on induction[33,34]. The average titre of retrovirus stocks prepared from these cell lines routinely exceeded approximately $1–10 \times 10^9$ inclusion-forming units per ml, as estimated using Jurkat cells.

Assays for anchorage-independent growth and tumorigenicity in nude mice. NIH3T3 cells (the Japan Cell Resource Bank) were stably transduced with wild-type and mutant *C-CBL* by retrovirus-mediated gene transfer. For colony formation assays, 1.0×10^3 stable cells for each construct were inoculated in 0.33% top agar, and the numbers of colonies >1 mm in diameter were counted 3 weeks after inoculation ($n = 8$). Experiments were repeated four times. For tumour formation in nude mice, 1.0×10^7 stable cells were inoculated subcutaneously at two sites per mouse. Cells were inoculated at six sites in three mice for each construct.

Purification of LSK HSPCs. LSK HSPCs were purified from bone marrow and spleen as described[35,36]. Multicolour flow cytometry analysis and cell sorting were performed using a MoFlo cell Sorter (Beckman Coulter). The purity of sorted cell fractions consistently exceeded 98%.

Replating assays of bone marrow progenitor cells. Bone marrow LSK cells were infected with IRES/GFP-containing retrovirus carrying mock, wild-type C-CBL and three C-CBL mutants (C-CBL(Gln367Pro), C-CBL(Tyr371Ser) and C-CBL(Cys384Gly)) as well as C-CBL(70Z) on RetroNectin-coated dishes. After 48 h infection in culture in StemSpan supplemented with SCF (50 ng ml^{-1}; Peprotech), TPO (20 ng ml^{-1}) and FLT3LG (20 ng ml^{-1}), 1.0×10^2 GFP-positive cells were inoculated in MethoCult M3231 supplemented with TPO (20 ng ml^{-1}), IL3 (10 ng ml^{-1}), IL6 (10 ng ml^{-1}), FLT3LG (10 ng ml^{-1}) and SCF (50 ng ml^{-1}) for colony formation. Colony-forming cells were collected 7 days after each inoculation, from which 1.0×10^3 cells were repeatedly subjected to replating until no colonies were produced. Experiments were repeated at the indicated times for each C-CBL construct.

Generation of *c-Cbl*$^{-/-}$ mice and evaluation of their tumour-prone phenotype. *c-Cbl*$^{-/-}$ mice were generated using a conventional method of gene targeting (Supplementary Fig. 10). *c-Cbl*$^{+/+}$, *c-Cbl*$^{+/-}$ and *c-Cbl*$^{-/-}$ mice were crossed with *BCR-ABL* transgenic mice, and their survival and the development of blastic crises were monitored.

Evaluation of haematopoietic pool size in *c-Cbl*$^{-/-}$ mice. LSK and CD34$^-$ LSK cells were sorted from bone marrow cells or spleens of *c-Cbl*$^{-/-}$ mice, and their numbers were compared to those in *c-Cbl*$^{+/+}$ littermates (8 week old). Approximately 5×10^5 bone marrow cells collected from *c-Cbl*$^{+/+}$ and *c-Cbl*$^{-/-}$ mice were inoculated into MethoCult M3231 culture supplemented with TPO (20 ng ml^{-1}), IL3 (10 ng ml^{-1}), IL6 (10 ng ml^{-1}), EPO (3 U ml^{-1}) and SCF (50 ng ml^{-1}). The number of colonies was counted 7 days after culturing.

***In vitro* cell proliferation assays.** Approximately 6×10^3 LSK cells from *c-Cbl*$^{-/-}$ mice and their *c-Cbl*$^{+/+}$ littermates (8 week old) were sorted into RetroNectin-coated 96-well U-bottom plates containing α-minimum essential medium supplemented with 1% fetal bovine serum (FBS), mouse SCF (50 ng ml^{-1}), and human TPO (100 ng ml^{-1}). After 24 h pre-incubation, retrovirus supernatant was added to each well at a multiplicity of infection of about 10. The plates were incubated for another 24 h in the presence of protamine sulphate (10 μg ml^{-1}), followed by repeated infection and extended culture for 2 days in S-Clone SF-O3 medium (Sanko Junyaku) supplemented with 1% BSA, 50 ng ml^{-1} SCF and 50 ng ml^{-1} TPO. On day 4, fluorescent-marker-positive cells were sorted for subsequent analyses. Cell survival and proliferation of LSK cells transduced with different *C-CBL* constructs were assessed in serum-free liquid culture in 96-well U-bottom plates in the presence of various cytokines. Each well received 50 fluorescent-marker-positive LSK cells, and the cells were cultured in S-Clone supplemented with 1% BSA plus SCF, TPO, IL3 or FLT3LG at the indicated concentrations. Cell numbers were counted either by analysing well images or by flow cytometry using FlowCount beads (Beckman Coulter). After 6 h serum starvation, 1×10^4 LSK cells transduced with various *C-CBL* constructs were stimulated with SCF (10 ng ml^{-1}) and TPO (10 ng ml^{-1}) for 15 min. Whole-cell lysates were examined for activation of STAT5 and Akt by immunoblots using the respective antibodies.

Immunoblot analysis of physical interactions between mutant C-CBL and CBL-B. Flag-tagged CBL-B or C-CBL was co-transfected into NIH3T3 cells with each of three HA-tagged C-CBL mutants (C-CBL(Gln367Pro), C-CBL(Tyr371Ser) and C-CBL(70Z)). Total cell lysates of these NIH3T3 cells were immunoprecipitated with anti-Flag antibody, followed by immunoblot analysis with anti-HA antibody.

Detection of ubiquitination and phosphorylation of kinases. After overnight serum starvation, NIH3T3 cells stably transduced with human EGFR, and indicated HA-tagged C-CBL mutants and Flag-tagged wild-type C-CBL were stimulated with human EGF (10 ng ml^{-1}) for 2 min. Cell lysates were immunoprecipitated with anti-EGF antibody, followed by immunoblotting using anti-ubiquitin antibody. Constructs for wild-type C-CBL and mutant C-CBL were stably transduced into a mast cell line, V3MC, FLT3-transduced 32D cells (32D/FLT3) and BaF3 cells transduced with human EPOR and JAK2 (BaF3/EPOR/JAK2) using retrovirus-mediated gene transfer. After overnight serum starvation, the transduced cells were stimulated with 10 ng ml^{-1} SCF (V3MC), 10 U ml^{-1} EPO (BaF3/EPOR/JAK2) or 10 ng ml^{-1} FLT3LG (32D/FLT3) for 1 min. The specific kinases were immunoprecipitated with relevant antibodies, and their ubiquitination was detected by immunoblotting with anti-ubiquitin antibody. Tyrosine phosphorylation of EGFR, c-KIT, JAK2 and FLT3 was examined by immunoblot analyses of total cell lysates after cytokine stimulation at indicated time points, using antibodies specifically recognizing phosphorylated kinases, anti-p-EGFR, anti-p-c-KIT, anti-p-JAK2 and anti-p-FLT3, respectively. Anti-GAPDH or anti-α-tubulin immunoblot was performed as a control. Antibodies used in this study are listed in Supplementary Table 9.

Statistical analysis. Statistical significance of prolonged replating capacity of mutant *C-CBL*-transduced LSK cells was tested by counting the total number of dishes that produced colonies, followed by Fisher's exact test. Survival curves of *c-Cbl*$^{+/+}$, *c-Cbl*$^{+/-}$ and *c-Cbl*$^{-/-}$ mice containing the *BCR-ABL* transgene were generated using the Kaplan–Meier method. Overall survivals of *C-CBL*-mutated and non-mutated CMML cases were analysed according to the proportional hazard model, using STATA software. Statistical differences in survival were evaluated using the log-rank test, and statistical differences in 2×2 contingency tables were tested according to Fisher's exact method. Student's *t*-tests were used to evaluate the significance of difference in spleen mass, number of haematopoietic progenitors and colony-forming cells between *c-Cbl*$^{+/+}$ and *c-Cbl*$^{-/-}$.

29. Blake, T. J. *et al.* The sequences of the human and mouse c-cbl proto-oncogenes show v-cbl was generated by a large truncation encompassing a proline-rich domain and a leucine zipper-like motif. *Oncogene* 6, 653–657 (1991).
30. Hamanaka, S. *et al.* Stable transgene expression in mice generated from retrovirally transduced embryonic stem cells. *Mol. Ther.* 15, 560–565 (2007).
31. Nabekura, T. *et al.* Potent vaccine therapy with dendritic cells genetically modified by the gene-silencing-resistant retroviral vector GCDNsap. *Mol. Ther.* 13, 301–309 (2006).
32. Sanuki, S. *et al.* A new red fluorescent protein that allows efficient marking of murine hematopoietic stem cells. *J. Gene Med.* 10, 965–971 (2008).
33. Ory, D. S., Neugeboren, B. A. & Mulligan, R. C. A stable human-derived packaging cell line for production of high titer retrovirus/vesicular stomatitis virus G pseudotypes. *Proc. Natl Acad. Sci. USA* 93, 11400–11406 (1996).
34. Suzuki, A. *et al.* Feasibility of *ex vivo* gene therapy for neurological disorders using the new retroviral vector GCDNsap packaged in the vesicular stomatitis virus G protein. *J. Neurochem.* 82, 953–960 (2002).
35. Ema, H. *et al.* Adult mouse hematopoietic stem cells: purification and single-cell assays *Nature Protoc.* 1, 2979–2987 (2006).
36. Osawa, M. *et al.* Long-term lymphohematopoietic reconstitution by a single CD34-low/negative hematopoietic stem cell. *Science* 273, 242–245 (1996).

Int J Hematol (2010) 91:97–103
DOI 10.1007/s12185-009-0473-4

ORIGINAL ARTICLE

Comparative analysis of remission induction therapy for high-risk MDS and AML progressed from MDS in the MDS200 study of Japan Adult Leukemia Study Group

Yasuyoshi Morita · Akihisa Kanamaru · Yasushi Miyazaki · Daisuke Imanishi · Fumiharu Yagasaki · Mitsune Tanimoto · Kazutaka Kuriyama · Toru Kobayashi · Shion Imoto · Kazunori Ohnishi · Tomoki Naoe · Ryuzo Ohno

Received: 12 August 2009 / Revised: 2 December 2009 / Accepted: 14 December 2009 / Published online: 5 January 2010

Abstract A total of 120 patients with high-risk myelodysplastic syndrome (MDS) and AML progressed from MDS (MDS–AML) were registered in a randomized controlled study of the Japan Adult Leukemia Study Group (JALSG). Untreated adult patients with high-risk MDS and MDS–AML were randomly assigned to receive either idarubicin and cytosine arabinoside (IDR/Ara-C) (Group A) or low-dose cytosine arabinoside and aclarubicin (CA) (Group B). The remission rates were 64.7% for Group A (33 of 51 evaluable cases) and 43.9% for Group B (29 out of 66 evaluable cases). The 2-year overall survival rates and disease-free survival rates were 28.1 and 26.0% for Group A, and 32.1 and 24.8% for Group B, respectively. The duration of CR was 320.6 days for Group A and 378.7 days for Group B. There were 15 patients who lived longer than 1,000 days after diagnosis: 6 and 9 patients in Groups A and B, respectively. However, among patients enrolled in this trial, intensive chemotherapy did not produce better survival than low-dose chemotherapy. In conclusion, it is necessary to introduce the first line therapy excluding the chemotherapy that can prolong survival in patients with high-risk MDS and MDS–AML.

For the Japan Adult Leukemia Study Group.

Y. Morita (✉) · A. Kanamaru
Department of Hematology,
Kinki University School of Medicine,
377-2 Ohno-Higashi,
Osaka-Sayama, Osaka 589-8511, Japan
e-mail: morita@int3.med.kindai.ac.jp

Y. Miyazaki · D. Imanishi
Department of Hematology, Molecular Medicine Unit,
Atomic Bomb Disease Institute, Nagasaki University
Graduate School of Biomedical Sciences, Nagasaki, Japan

F. Yagasaki
Department of Hematology,
Saitama Medical University Hospital, Saitama, Japan

M. Tanimoto
Blood Transfusion Division, Department of Internal
Medicine II, Okayama University Graduate School
of Medicine and Dentistry, Okayama, Japan

K. Kuriyama
Blood Immunology Laboratory, School of Health Sciences,
Faculty of Medicine and University Hospital,
University of the Ryukyus, Okinawa, Japan

T. Kobayashi
Department of Hematopoietic Pathobiology
and Medical Oncology,
Mie University Graduate School of Medicine,
Tsu, Japan

S. Imoto
Hyogo Prefectural Red Cross Blood Center,
Hyogo, Japan

K. Ohnishi
Third Department of Internal Medicine,
Hamamatsu University School of Medicine,
Hamamatsu, Japan

T. Naoe
Department of Hematology and Oncology,
Nagoya University Graduate School of Medicine,
Nagoya, Japan

R. Ohno
Aichi Cancer Center, Aichi, Japan

Keywords MDS · MDS–AML · JALSG MDS200 · Induction therapy · HSCT

1 Introduction

Myelodysplastic syndrome (MDS) is a group of disorders in which abnormalities occur at the level of hematopoietic stem cells [1], leading to disturbance in the production of blood cells characterized by ineffective hematopoiesis [2], decrease in the number of peripheral blood cells and morphological/functional abnormalities in blood cells [3]. Allogeneic hematopoietic cell transplantation (allo-HCT) is the most effective curative therapy for acute myeloid leukemia (AML) and myelodysplastic syndromes (MDS) [4]. However, for patients with high-risk MDS (those with refractory anemia with excess of blasts in transformation (RAEB)-t and some patients with RAEB) and patients with acute myeloid leukemia progressed from MDS (MDS–AML), chemotherapy aimed at remission is being used. The reasons for this are that MDS often affects elderly people [5], suitable donors are not always available at the time of disease onset, the necessity of pretransplant conditioning chemotherapy is controversial [6, 7] with a lack of sufficient evidence, and the optimal timing for transplantation varies widely depending on disease type [8].

On the other hand, reduced-intensity conditioning has extended the use of allo-HSCT to patients otherwise not eligible for this treatment due to older age or frailty [9]. However, allo-HSCT using traditional myeloablative preparative regimens is not easily tolerated by the elderly or frailer patient, and may lead to prohibitive treatment-related mortality rates. Most patients treated in the past were younger and devoid of comorbid clinical conditions. Novel reduced-intensity regimens have recently made allogeneic transplants applicable to the elderly, providing the benefit of the graft-versus-leukemia effect to a larger number of patients in need [10].

Low-dose chemotherapy, which has been used in clinical practice for 20 years, reduces the number of myeloblasts, improves pancytopenia and induces remission not only in MDS patients but also in some MDS–AML patients [11]. Common antineoplastic agents used in low-dose chemotherapy include cytosine arabinoside (Ara-C), aclarubicin (ACR), melphalan and etoposide. Nevertheless, despite improved Ara-C and regimens, the prognosis of AML in patients beyond 60 years of age remains dismal [4]. Low-dose antineoplastic drug therapy is still being used in some patients with MDS, which is common in elderly people, especially when the patient is at risk due to poor general condition or organ disorder [12].

The Japan Adult Leukemia Study Group (JALSG) previously conducted a pilot study for the treatment of high-risk MDS and MDS–AML to compare low-dose monotherapy with low-dose Ara-C plus granulocyte colony-stimulating factor (G-CSF) and multiple drug therapy with Ara-C plus Mitoxantrone plus VP-16. Later, JALSG conducted studies using a single protocol (JALSG MDS96) in 1996, in which remission induction and post-remission therapies using Ara-C and IDR in patients with high-risk MDS (RAEB-t) and in those with MDS–AML were performed, after which the efficacy and safety of these therapies were evaluated [13]. Furthermore, a randomized controlled study (JALSG MDS200) of intensive chemotherapy (IDR/Ara-C) or low-dose chemotherapy (CA) for high-risk MDS was also performed by JALSG.

Here, we present and analyze the results of the JALSG MDS200 study to assess and evaluate the validity of the MDS200 protocol for MDS treatment.

2 Patients and methods

2.1 Patient eligibility

A total of 120 patients were initially registered into the JALSG MDS200 study between June 2000 and March 2005. They were assigned into two groups, namely, Groups A and B (Table 1). Patients aged 15 years or more and diagnosed as having high-risk RAEB with high International Prognostic Scoring System score [14], RAEB-t or MDS-AML were eligible for this study. MDS–AML denotes secondary AML transformed from MDS.

Other eligibility criteria were as follows: patients with a performance status (PS) of 0–2 (ECOG); patients whose key organs other than the bone marrow retain intact function; patients who have not undergone any chemotherapy, except for pretreatment that does not affect the outcome of the main therapy; and patients who have given informed consent. Informed consent was obtained after carefully explaining the protocol and before registration.

2.2 Study protocol

The MDS200 protocol (Fig. 1) was designed based on the results of MDS96, and involved a dose-attenuation plan and allowed a wider range of chemotherapy. Patients were randomly assigned to either Group A or B.

In therapy A, the dose was adjusted according to a dose attenuation plan based on the presence of risk factors. The following 3 factors were regarded as risk factors: (1) Age ($\geq$60 years), (2) hypoplastic bone marrow and (3) PS $\geq$ 2. Patients with no risk factor received the standard dose, those with 1 risk factor received 80% of the dose and those with 2 or more risk factors received 60% of the dose (equivalent to the dose of MDS96). In therapy B, the use of

Table 1 Characteristics of patients

Group	A ($n = 53$)	B ($n = 67$)	P value (A vs. B)
Age (range)	63 (23–77)	61 (32–81)	0.505
Gender			
Male	37	52	0.332
Female	16	15	
Disease type			
HR-RAEB	4	11	0.269
RAEB-T	22	29	
MDS–AML	27	27	
Infection			
Presence	10	11	0.726
None	43	56	
Karyotype[a]			
Good	23 (44.2%) $n = 52$	21 (33.9%) $n = 62$	0.524
Int	11 (21.2%)	15 (24.2%)	
Poor	18 (34.6%)	26 (41.9%)	
PB (range)			
WBC (/μL)	2,500 (700–64,240)	2,720 (600–43,700)	0.665
Hb (g/dL)	8 (4.7–12.6)	7.9 (4.4–12.7) $n = 66$	0.562
Plt (/μL)	5.8 (0.2–31.4)	5.9 (0.5–36.7)	0.363
BM (range)			
Blast (%)	30 (4–95) $n = 51$	24.2 (1.9–96) $n = 66$	0.171
Biochemical data (range)			
LDH (IU/L)	296 (132–882)	303.5 (111–906) $n = 66$	0.998
CRP (mg/dL)	0.5 (0–20.2)	0.35 (0–11.7) $n = 66$	0.292

Patients who met all of the inclusion criteria and did not meet any of the stated exclusion criteria were included the study. The disease types were classified by FAB classification

Statistical analysis between Group A and Group B was done using χ^2 test or Mann–Whitney U-test

MDS myelodysplastic syndrome, *HR-RAEB* high risk-refractory anemia excess of blasts with high International Prognostic Scoring System Score, *RAEB-T* refractory anemia excess of blasts in transformation, *MDS–AML* MDS overt leukemia, *WBC* white blood cell, *Hb* hemoglobin, *Plt* platelet, *LDH* lactate dehydrogenase, *CRP* C-reactive protein, *PB* peripheral blood, *BM* bone marrow

[a] Shows IPSS risk

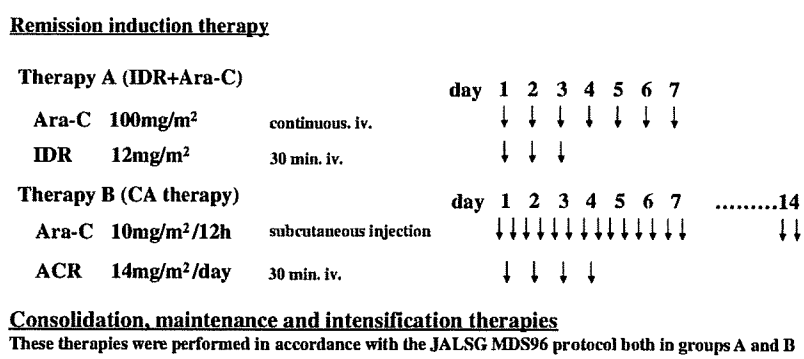

Fig. 1 Japan Adult Leukemia Study Group—myelodysplastic syndrome (JALSG MDS200 Protocol). In therapy A, the dose was adjusted according to a dose attenuation plan based on the presence of risk factors. The following 3 factors were regarded as risk factors: (1) Age (≥60 years), (2) hypoplastic bone marrow and (3) PS ≥ 2. Patients with no risk factor received the standard dose, those with 1 risk factor received 80% of the dose, and those with 2 or more risk factors received 60% of the dose (equivalent to the dose of MDS-96). In therapy B, the use of CAG therapy involving co-administration of G-CSF was allowed. *IDR* idarubicin, *Ara-C* cytosine arabinoside, *ACR* aclarubicin, *G-CSF* granulocyte colony-stimulating factor, *iv* intravenous injection, *min* minutes

CAG therapy involving the co-administration of granulocyte colony-stimulating factor (G-CSF) was allowed.

Untreated adult patients (≥15 years) with MDS (RAEB, RAEB-t or MDS–AML) were randomly assigned to receive either IDR/Ara-C (Group A) or CA (Group B) [15]. Complete remission (CR) rate, CR duration, overall survival (OS) rate and disease-/relapse-free survival (DFS/RFS) rate were compared between the two groups.

Consolidation therapy and maintenance therapy were performed in accordance with JALSG MDS96 [13].

2.3 Evaluation of response

Response to treatment was evaluated in accordance with JALSG criteria [13]. CR was considered achieved when the following conditions remained for at least 4 weeks. For the bone marrow: blasts accounting for ≤5% of all cells; absence of blasts with Auer body; and presence of normal erythroblasts, granulocytes and megakaryocytes. For peripheral blood: absence of blasts; neutrophils ≥ 1,000/ml; platelets ≥ 100,000/μL; and no evidence of extramedullary leukemia. CR duration was defined as the duration from the day when CR is achieved to the day of relapse or death, OS or DFS as the duration from the day of initiation of treatment to the day of death and DFS as the duration in which CR patients survived without relapse. Patients who were treated with HCST were not censored at the date of transplantation. All toxicity was graded using the World Health Organization criteria [16].

2.4 Statistical analysis

The primary endpoint of this study is DFS. Assuming a 1-year DFS rate of 60% in the Group A and 40% in the Group B, this design required the randomization of 200 patients. Eligible patients were randomized according to age, sex and disease type. Differences in background factors (e.g., age, gender and disease type) between Groups A and B were statistically analyzed using the χ^2 test or Mann–Whitney U-test. Probability of OS and DFS were estimated according to the method of Kaplan and Meier.

3 Results

3.1 Recruitment of patients and suspension of the study

The initially registered 120 patients were assigned into two groups, namely, Groups A and B. The clinical characteristics of the registered patients are shown in Table 1. The present protocol was originally planned to recruit 200 patients for Groups A and B within 3 years. However, the recruitment pace was slower than expected and thus the study period was extended from 3 years to 4.5 years. At the end of 2004, that is, after 4.5 years from the start of the study, the number of registered patients was only 113 in Groups A and B, which was 56.5% of the target number. At that point, the committee members discussed the progress of the MDS200 study and decided to suspend it at the end of March 2005. Since the final total number of patients did not reach the target number, we did not statistically compare DFS between Groups A and B, which was the primary endpoint of this study.

3.2 Characteristics of patients

There were no clear differences in the clinical characteristics of the patients between Groups A and B, such as FAB subtype, initial blood cell count, presence of infection, distribution in the karyotype group and biochemical data, as well as sex distribution (male/female ratio, 37/16 = 2.315 in Group A, and 52/15 = 3.467 in Group B).

3.3 Treatment outcome

The remission rates were 64.7% in Group A (33 out of 51 evaluable cases) and 43.9% in Group B (29 out of 66 evaluable cases). The 2-year overall survival (OS) rates were 28.1% in Group A and 32.1% in Group B, and the 2-year DFS rates were 26.0% in Group A and 24.8% in Group B. The mean duration of CR was 320.6 days (median: 213 days) in Group A and 378.7 days (median: 273 days) in Group B (Table 2). Reflecting the intensity of the remission induction chemotherapy, the period of WBC (<1,000/μL) after the therapy was longer in Group A than in Group B (19 days and 4 days, respectively). There were more grade 3 or 4 adverse events during the remission induction therapy in Group A (19 out of 53 evaluable patients) than in Group B (13 out of 67 evaluable patients). This difference was mostly attributable to infectious episodes (17 patients in Group A and 4 patients in Group B). In terms of bleeding episodes, 1 patient in Group A and 2 in Group B had grade 3/4 adverse events. The numbers of

Table 2 Treatment outcome (Group A vs. B)

	Group A ($n = 53$)	Group B ($n = 67$)
Remission rate (%)	64.7	43.9
Mean duration of remission (days)	320.6 (median: 213)	378.7 (median: 273)
2-Year survival rate (%)	28.1	32.1
2-Year disease-free survival rate (%)	26.0	24.8

The remission rates, 2-year overall survival (OS) rates and 2-year disease-free survival (DFS) rates are shown as percentages

early death in remission induction chemotherapy (death within 30 days) were 1 patient in Group A and 3 patients in Group B (Table 3). The cause of death in each group was infection or tumor progression. The completion rate of consolidation therapies were 37.3% in Group A (12 out of 33 evaluable cases), 37.9% in Group B (11 out of 29 evaluable cases). On the other hand, the maintenance therapies were completed 21.2% in Group A (7 out of 33 evaluable cases), and 15.2% in Group B (5 out of 33 evaluable cases). The numbers of dose attenuation in Group A were 30 patients of 100% dose, 21 patients of 80% or 60% dose and 2 patients of unknown.

Allogeneic hematopoietic stem cell transplantation (allo-HSCT) was performed in 11 out of 50 patients (22%) in Group A and 19 out of 66 patients (28.8%) in Group B. Among those who received allo-HSCT, the transplantation was performed during the first remission in 40%, 21% of patients in Groups A, B, respectively.

There were 15 patients who lived longer than 1,000 days after diagnosis: 6, 9 patients in Groups A, B, respectively. Regarding the transplantation among long-term survivors, 3 out of 6 patients were transplanted in Group A, 6 out of 9 in Group B. Comparing the achievement of CR among these patients in Groups A and B, all 6 patients in Group A achieved CR, but only 4 out of 9 patients in Group B achieved CR.

Table 3 Toxicity of the induction therapy

	A ($n = 53$) (range)	B ($n = 67$) (range)	P value (A vs. B)
Period of WBC <1,000 (day)	19 (0–44) $n = 49$	4 (0–50) $n = 63$	<0.0001
Toxicity (grade 3/4)			
Presence	19	13	0.427
Bleeding	2	1	ND
Infection	17	11	0.04
Others	2	2	ND
Early death (<30 days)	1	3	ND

Statistical analysis between Groups A and B was performed using the χ^2 test or Mann–Whitney U-test

ND not done

4 Discussion

In this MDS200 study, patients with high-risk MDS and AML transformed from MDS (MDS–AML) were treated with either intensive or low-dose remission induction therapy, followed by intensive post-remission therapy that was the same as in the JALSG MDS96 study [13].

Although we did not perform statistical comparison of DFS or OS between these two treatment groups due to the insufficient number of patients enrolled, the results suggest that there was no significant difference, that is, survival curves were superimposable (Figs. 2, 3). Intensive chemotherapy similar to that for AML can produce a CR rate of 64.7% for high-risk MDS and MDS–AML patients, whereas low-dose induction therapy can result in a CR rate of 43.9%. However, among the patients enrolled in this trial, the difference in CR rate did not lead to better survival as described above. In terms of adverse events, patients who received intensive treatment had more grade 3 or 4 adverse events, particularly infectious events with a longer period of leukopenia. There was no increase in the number of patients succumbing to early death (death within 30 days after the

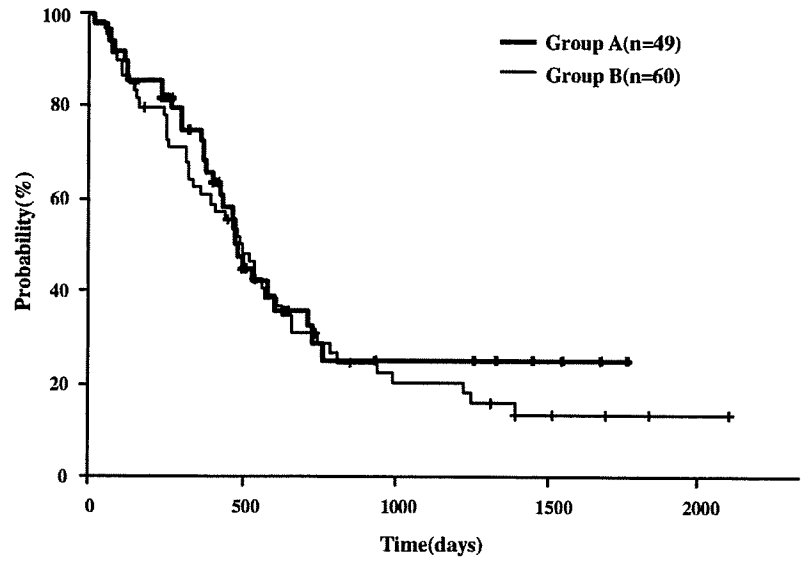

Fig. 2 Overall survival. Survival was calculated from the date of the start of treatment to the date of death due to any cause or to the date of the most recent follow-up. These data were not censored at the time of HSCT. All randomized patients were not included this data in each group. Due to this reason, some patients were not known to be CR or not, but known to be alive or not

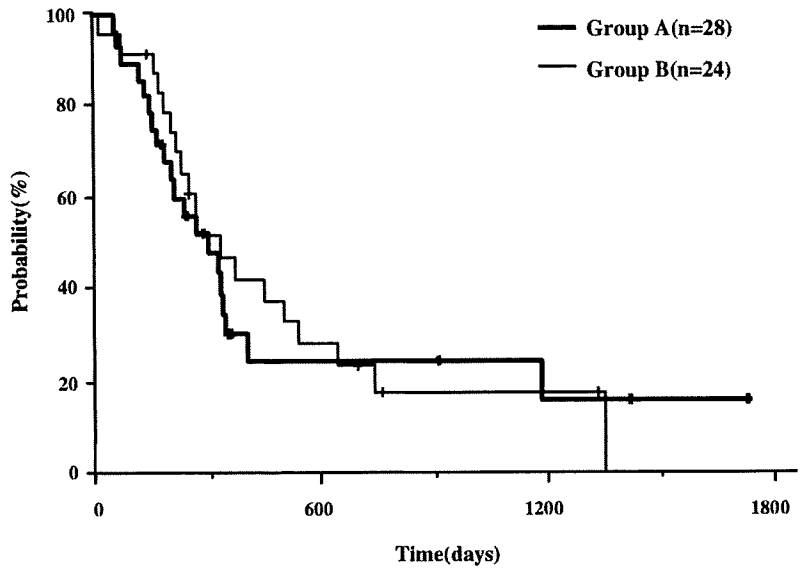

Fig. 3 Disease-/relapse-free survival. RFS was calculated from the date of achieving complete remission to the date of relapse, death or the most recent follow-up. These data were not censored at the time of HSCT. All randomized patients were not included this data in each group. Due to this reason, some patients were not known to be CR state or relapse, but known to be alive or not

start of treatment) in Group A, suggesting that intensive treatment produced higher CR rate, and higher toxicity resulted in a similar survival rate with low-dose induction therapy at least during the early phase of treatment.

There are several reasons that could explain why no difference in survival rate was observed regardless of the difference in CR rate. One could be the similar post-remission therapy between Groups A and B, as demonstrated by the almost similar DFS curves among the two groups. Another reason could be the disease status at the time of transplantation for patients in the two groups. In Group A, 60% of the transplantation was performed during the period other than that covering the first CR; this was 79% in Group B. Allo-HSCT has been shown to have the strongest antileukemia effect, and this was also found in the current study in which 6 out of 15 long-term survivors received allo-HSCT in Groups A and B. From the viewpoint of transplantation, intensive treatment merely selected cases that were suitable for transplantation, as observed in the case of transplantation for relapsed AML patients [17]. There are arguments against remission induction therapy for MDS patients in that it does not affect post-transplant prognosis [6, 18]. In the results of JSHCT, the chemotherapy before undergoing allo-SCT is not necessary in patients with MDS [6]. A group from the Institute of Medical Science of Tokyo University performed umbilical cord blood stem cell transplantation without remission induction therapy in high-risk MDS patients aged not more than 55 years and obtained favorable results with reduced time from diagnosis to transplantation [19]. It is important to perform clinical studies based on the concept that HCST should be performed immediately after diagnosis without remission induction, and determine the types of patients who would benefit from remission induction therapy prior to transplantation in terms of prognosis. In the present study, although suspended because of the insufficient number of patients enrolled, it appears that remission induction therapy with IDR and Ara-C did not produce better survival than that with low-dose chemotherapy despite higher CR rate. Therefore, it is suggested that CR rate is not a suitable surrogate marker for the evaluation of the outcome of chemotherapy for high-risk MDS and MDS–AML. In the latest reports, induction chemotherapy for patients with high-risk MDS and MDS–AML also provide no survival advantage [20, 21]. Considering the low survival rate of patients in this category, it is clearly necessary to introduce new strategies for the treatment of high-risk MDS and MDS–AML, such as molecular targeting agents and allo-HSCT with reduced-intensity conditioning regimens.

Acknowledgments We would like to thank the participating physicians in the Japan Adult Leukemia Study Group (JALSG) MDS200 study for their cooperation. This work was supported in part by grants-in-aid for Scientific Research from the Japanese Ministry of Education, Culture, Sport, Science, and Technology, and grants-in-aid for Cancer Research from the Japanese Ministry of Health, Labor, and Welfare.

References

1. Mhawech P. Myelodysplastic syndrome: review of the cytogenetic and molecular data. Crit Rev Oncol/Hematol. 2001;40:229–38.
2. Hofmann W, Koeffler HP. Myelodysplastic syndrome. Ann Rev Med. 2005;56:1–16.
3. Bennett JM, Catovsky D, Daniel MT, Flandrin G, Galton DA, Gralnick HR, et al. Proposals for the classification of the myelodysplastic syndromes. Br J Haematol. 1982;51:189–99.

4. Finke J, Nagler A. Viewpoint: what is the role of allogeneic haematopoietic cell transplantation in the era of reduced-intensity conditioning—is there still an upper age limit? A focus on myeloid neoplasia. Leukemia. 2007;21:1357–62.
5. Tricot GJ. Prognostic factors in myelodysplastic syndrome. Leuk Res. 1992;16:109–15.
6. Nakai K, Kanda Y, Fukuhara S, Sakamaki H, Okamoto S, Kodera Y, et al. Value of chemotherapy before allogeneic hematopoietic stem cell transplantation from an HLA-identical sibling donor for myelodysplastic syndrome. Leukemia. 2005;19:396–401.
7. De Witte T. Stem cell transplantation for patients with myelodysplastic syndrome and secondary leukemias. Int J Hematol. 2000;72:151–6.
8. Cutler CS, Lee SJ, Greenberg P, Deeg HJ, Perez WS, Anasetti C, et al. A decision analysis of allogeneic bone marrow transplantation for the myelodysplastic syndrome: delayed transplantation for low risk myelodysplasia is associated with improved outcome. Blood. 2004;104:579–85.
9. Oran B, Giralt S, Saliba R, Hosing C, Popat U, Khouri I, et al. Allogeneic hematopoietic stem cell transplantation for the treatment of high-risk acute myelogenous leukemia and myelodysplastic syndrome using reduced-intensity conditioning with fludarabine and melphalan. Biol Blood Marrow Transplant. 2007;13:454–62.
10. Lekakis L, de Lima M. Reduced-intensity conditioning and allogeneic hematopoietic stem cell transplantation for acute myeloid leukemia. Expert Rev Anticancer Ther. 2008;8:785–98.
11. Denzlinger C, Bowen D, Benz D, Gelly K, Brugger W, Kanz L. Low-dose melphalan induces favourable responses in elderly patients with high-risk myelodysplastic syndromes or secondary acute leukaemia. Br J Haematol. 2000;108:93–5.
12. Miller KB, Kim K, Morrison FS, Winter JN, Bennett JM, Neiman RS, et al. The evaluation of low-dose cytarabine in the treatment of myelodysplastic syndrome. Ann Hematol. 1992;65:162–8.
13. Okamoto T, Kanamaru A, Shimazaki C, Motoji T, Takemoto Y, Takahashi M, et al. Combination chemotherapy with risk factor-adjusted dose attenuation for high-risk myelodysplastic syndrome and resulting leukemia in the multicenter study of the Japan Adult Leukemia Study Group (JALSG): results of an interim analysis. Int J Hematol. 2000;72:200–5.
14. Greenberg P, Cox C, LeBeau MM, Fenaux C, Morel P, Sanz G, et al. International scoring system for evaluating progenitors in myelodysplastic syndrome. Blood. 1997;89:2079–88.
15. Yamada K, Furusawa S, Saito K, Waga K, Koike T, Arimura H, et al. Concurrent use of granulocyte colony-stimulating factor with low-dose cytosine arabinoside and aclarubicin for previously treated acute myelogenous leukemia: a pilot study. Leukemia. 1995;9:10–4.
16. Miller AB, Hoogstraten B, Staquet M, Winkler A. Reporting results of cancer treatment. Cancer. 1981;47:207–14.
17. Alessandrino EP, Della Porta MG, Bacigalupo A, Van Lint MT, Falda M, Onida F, et al. WHO classification and WPSS predict post-transplantation outcome in patients with myelodysplastic syndrome: a study from the Gruppo Italiano Trapianto di Midollo Osseo (GITMO). Blood. 2008;112:895–902.
18. Nachtkamp K, Kundgen A, Strupp C, Giagounidis A, Kobbe G, Gattermann N, et al. Impact on survival of different treatments for myelodysplastic syndromes (MDS). Leuk Res. 2009;33:1024–8.
19. Ooi J. The efficacy of unrelated cord blood transplantation for adult myelodysplastic syndrome. Leuk Lymphoma. 2006; 47:599–602.
20. Knipp S, Hildebrand B, Kundgen A, Giagounidis A, Kobbe G, Haas R, et al. Intensive chemotherapy is not recommended for patients aged >60 years who have myelodysplastic syndromes or acute myeloid leukemia with high-risk karyotypes. Cancer. 2007;110:345–51.
21. Fenaux P, Mufti GJ, Hellstrom-Lindberg E, Santini V, Finelli C, Giagounidis A, et al. Efficacy of azacitidine compared with that of conventional care regimens in the treatment of higher-risk myelodysplastic syndromes: a randomized, open-rabell, phase III study. Lancet Oncol. 2009;10:223–32.

THE JOURNAL OF BIOLOGICAL CHEMISTRY VOL. 285, NO. 3, pp. 1850–1860, January 15, 2010

Up-regulation of Survivin by the E2A-HLF Chimera Is Indispensable for the Survival of t(17;19)-positive Leukemia Cells*

Received for publication, June 10, 2009, and in revised form, October 29, 2009 Published, JBC Papers in Press, November 2, 2009, DOI 10.1074/jbc.M109.023762

Mayuko Okuya[‡], Hidemitsu Kurosawa[‡1], Jiro Kikuchi[§], Yusuke Furukawa[§], Hirotaka Matsui[¶], Daisuke Aki[¶], Takayuki Matsunaga[‡], Takeshi Inukai[‖], Hiroaki Goto[**], Rachel A. Altura[‡‡], Kenich Sugita[‡], Osamu Arisaka[‡], A. Thomas Look[§§], and Toshiya Inaba[¶]

From the [‡]Department of Pediatrics, Dokkyo Medical University School of Medicine, Tochigi 321-0293, Japan, the [§]Division of Stem Cell Regulation Center for Molecular Medicine, Jichi Medical School, Tochigi 329-0498, Japan, the [¶]Department of Molecular Oncology, Research Institute for Radiation Biology and Medicine, Hiroshima University, Hiroshima 734-8553, Japan, the [‖]Department of Pediatrics, University of Yamanashi School of Medicine, Yamanashi 409-3898, Japan, the [**]Department of Pediatrics, Yokohama City University School of Medicine, Kanagawa 236-0004, Japan, the [‡‡]Department of Pediatrics, The Warren Alpert Medical School of Brown University, Providence, Rhode Island 02903, and the [§§]Pediatric Oncology Department, Dana-Farber Cancer Institute, Boston, Massachusetts 02115

The E2A-HLF fusion transcription factor generated by t(17;19)(q22;p13) translocation is found in a small subset of pro-B cell acute lymphoblastic leukemias (ALLs) and promotes leukemogenesis by substituting for the antiapoptotic function of cytokines. Here we show that t(17;19)$^+$ ALL cells express Survivin at high levels and that a dominant negative mutant of E2A-HLF suppresses Survivin expression. Forced expression of E2A-HLF in t(17;19)$^-$ leukemia cells up-regulated Survivin expression, suggesting that Survivin is a downstream target of E2A-HLF. Analysis using a counterflow centrifugal elutriator revealed that t(17;19)$^+$ ALL cells express Survivin throughout the cell cycle. Reporter assays revealed that E2A-HLF induces *survivin* expression at the transcriptional level likely through indirect down-regulation of a cell cycle-dependent *cis* element in the promoter region. Down-regulation of Survivin function by a dominant negative mutant of Survivin or reduction of Survivin expression induced massive apoptosis throughout the cell cycle in t(17;19)$^+$ cells mainly through caspase-independent pathways involving translocation of apoptosis-inducing factor (AIF) from mitochondria to the nucleus. AIF knockdown conferred resistance to apoptosis caused by down-regulation of Survivin function. These data indicated that reversal of AIF translocation by Survivin, which is induced by E2A-HLF throughout the cell cycle, is one of the key mechanisms in the protection of t(17;19)$^+$ leukemia cells from apoptosis.

The E2A-HLF fusion transcription factor, which is generated by the t(17;19)(q22;p13) translocation, is found in a small subset of pro-B cell acute lymphoblastic leukemias (ALLs)[2] that occurs in older children and adolescents (1, 2). In this chimeric molecule, the *trans*-activation domain of E2A is fused to the basic region and leucine zipper domain of HLF, which mediates DNA binding and dimerization. Patients with this chimera share distinct clinical features such as hypercalcemia and coagulopathy and very poor prognosis because of resistance to intensive chemotherapy, including aggressive conditioning for bone marrow transplantation (3–5), all of which are unusual for pro-B cell ALLs. Thus, these features may be a direct consequence of aberrant gene expression induced by E2A-HLF fusion transcription factor, rather than a consequence of the nature of B cell progenitors.

We previously demonstrated that inhibition of the *trans*-activation potential of the E2A-HLF chimera by a dominant negative mutant results in apoptosis in t(17;19)$^+$ ALL cells but does not affect the cell cycle (6). Moreover, E2A-HLF blocks apoptosis normally induced by cytokine deprivation in murine interleukin (IL)-3-dependent B precursor lines such as Baf-3 or FL5.12 cells, suggesting that this fusion protein contributes to leukemogenesis through modification of apoptosis regulatory pathways normally controlled by cytokines (6, 7). We speculated that the target genes of E2A-HLF involved in the inhibition of apoptosis are those regulated via Ras pathways in IL-3-dependent cells, because activation of Ras pathways is indispensable for long term survival of Baf-3 cells in cytokine-free medium (8, 9). Moreover, we previously identified E4BP4/NFIL3, a related basic region and leucine zipper factor with antiapoptotic function, as a possible physiological counterpart of E2A-HLF (10), and we found that E4BP4 expression is induced by IL-3 through Ras-phosphatidylinositol 3-kinase and Ras-Raf-MAPK pathways in IL-3-dependent cells (9).

The *survivin* gene may be a good candidate for a target gene of E2A-HLF involved in the inhibition of apoptosis in t(17;19)$^+$

* This work was supported by Grant-in-aid for Scientific Research (C) 18591201 from the Japan Society for Promotion of Science (to H. K.) and a young investigator award from Dokkyo Medical University (to M. O.).

[1] To whom correspondence should be addressed: Dept. of Pediatrics, Dokkyo Medical University, Mibu, Tochigi 321-0293, Japan. Tel.: 81-282-86-1111; Fax: 81-282-86-2947; E-mail: hidekuro@dokkyomed.ac.jp.

[2] The abbreviations used are: ALL, acute lymphoblastic leukemia; AIF, apoptosis-inducing factor; IL, interleukin; MAPK, mitogen-activated protein kinase; CHR, cell cycle homology region; PBS, phosphate-buffered saline; FITC, fluorescein isothiocyanate; shRNA, short hairpin RNA; siRNA, short interfering RNA; GFP, green fluorescent protein; EMSA, electrophoretic mobility shift assay; BrdUrd, bromodeoxyuridine; TdT, terminal deoxynucleotidyltransferase; PARP, poly(ADP-ribose) polymerase; TUNEL, terminal deoxynucleotidyltransferase-mediated dUTP nick-end-labeling; PI, propidium iodide; dn, dominant negative; nt, nucleotide; 7-AAD, 7-amino-actinomycin D; PLL, plenti-Lox3.7.

ALL cells. Survivin, at 142 amino acids, is the smallest member of the inhibitor of apoptosis protein family and significantly prolongs the viability of cytokine-deprived IL-3-dependent cells (11). The expression of Survivin is controlled by oncogenic c-H-ras, and up-regulation of Survivin depends on functional Ras/phosphatidylinositol 3-kinase and Ras-Raf-MAPK signaling pathways (12). Overexpression of Survivin can protect cells from both extrinsically and intrinsically induced apoptosis (13, 14), whereas inhibition of Survivin expression by antisense ribozyme or RNA interference leads to increased spontaneous apoptosis (15, 16).

A unique feature of Survivin as an apoptosis regulator is its involvement in cell cycle progression (17). *survivin* expression is transcriptionally induced in the G_2/M phase through cell cycle-dependent *cis* elements located near the transcription initiation site (16). These elements, including the cell cycle-dependent element (GGCGG) and the cell cycle homology region (CHR; ATTTGAA), are implicated in G_1 transcriptional repression in S/G_2-regulated genes, such as cyclin A, cdc25C, and cdc2 (18). In addition, Survivin is activated through phosphorylation of Thr-34 by mitotic kinase CDC2-cyclin-B1 (14). Enforced expression of a phosphorylation-defective Survivin T34A mutant (Survivin-T34A) initiates mitochondrial dependent apoptosis in a variety of tumor cell lines (14, 16).

Here, we show that Survivin expression is induced by the E2A-HLF chimera, and down-regulation of Survivin induces caspase-independent massive apoptosis in t(17;19)$^+$ ALL cell lines. These findings indicate that Survivin contributes to leukemogenesis by subverting genetic pathways responsible for the apoptosis of B cell progenitors.

EXPERIMENTAL PROCEDURES

Cell Lines and Cell Culture—Human ALL cell lines that express E2A-HLF (UOC-B1, HAL-01, YCUB-2, and Endo-kun) and other leukemia cell lines (Nalm-6, RS4;11, REH, 697, 920, HL-60, NB-4, and Jurkat) were cultured in RPMI 1640 medium containing 10% fetal bovine serum. Establishment of Nalm-6 human pro-B cell leukemia cells that express zinc-inducible E2A-HLF (Nalm-6/E2A-HLF) using the pMT-CB6$^+$ eukaryotic expression vector (a gift from Dr. F. Rauscher III, Wistar Institute, Philadelphia) has been described previously (19). UOC-B1/E2A-HLF(dn) cells transfected with a dominant negative mutant of E2A-HLF, which lacks the AD1 transactivation domain of E2A and contains a mutated HLF DNA-binding domain with an intact leucine-zipper domain, were prepared as described previously (6). UOC-B1, Endo-kun, REH, and Jurkat cells that were transfected with either the pMT/Survivin-T34A vector or the empty pMT-CB6$^+$ vector were designated as UOC-B1/Survivin(dn), UOC-B1/pMT, Endo-kun/Survivin(dn), Endo-kun/pMT, REH/Survivin(dn), REH/pMT, Jurkat/Survivin(dn), and Jurkat/pMT, respectively.

Counterflow Centrifugal Elutriations—Counterflow centrifugal elutriations were performed using the SRR6Y elutriation system and rotor equipped with a 4.5-ml chamber (Hitachi Koki Co., Ltd., Tokyo, Japan) (20). Target cells were resuspended at 1–2 × 10^8 cells in 50 ml of PBS containing 1% fetal bovine serum and injected into the elutriation system at 4 °C using an initial flow rate of 16 ml/min and rotor speed of 2,000 rpm. The flow rate was incrementally increased, and cell fractions were collected serially as follows: fraction 1, 200 ml at 16 ml/min; fraction 2, 200 ml at 18 ml/min; fraction 3, 200 ml at 20 ml/min; fraction 4, 200 ml at 22 ml/min; fraction 5, 200 ml at 24 ml/min; fraction 6, 200 ml at 26 ml/min; and fraction 7, 200 ml at 28 ml/min. Cell cycle analysis was performed on each fraction by staining DNA with propidium iodide (PI) in preparation for flow cytometry with the FACScan/CellFIT system (BD Biosciences).

Gene Silencing by RNA Interference—Short hairpin/short interfering RNA (shRNA/siRNA) was introduced into UOC-B1 or UOC-B1/Survivin(dn) cells to down-regulate the expression of Survivin or apoptosis-inducing factor (AIF) by the shRNA lentivirus system (21, 22). Oligonucleotides were chemically synthesized, annealed, terminally phosphorylated, and inserted into the vector pLL3.7 (Addgene, Cambridge, MA). Oligonucleotides containing siRNA target for *survivin* sequences (23) were as follows: 5′-TGAAGCGTCTGGCAGATACTTTCAAGAGAAGTATCTGCCAGACGCTTCTTTTTTC-3′ (forward 1) and 5′-TCGAGAAAAAAGAAGCGTCTGGCAGATACTTCTCTTGAAAGTATCTGCCAGACGTTCA-3′ (reverse 1); 5′-TGTGGATGAGGAGACAGAATTTCAAGAGAATTCTGTCTCCTCATCCACTTTTTTC-3′ (forward 3) and 5′-TCGAGAAAAAAGTGGATGAGGAGACAGAATTCTCTTGAAATTCTGTCTCCTCATCCACA-3′ (reverse 3); 5′-TGGATACTTCACTTTAATAATTCAAGAGATTATTAAAGTGAAGTATCCTTTTTTTC-3′ (forward 4) and 5′-TCGAGAAAAAAGGATACTTCACTTTAATAATCTCTTGAATTATTAAAGTGAAGTATCCA-3′ (reverse 4); 5′-TGCTTCCTCGACATCTGTTATTCAAGAGATAACAGATGTCGAGGAAGCTTTTTTTC-3′ (forward 5) and 5′-TCGAGAAAAAAGCTTCCTCGACATCTGTTATCTCTTGAATAACAGATGTCGAGGAAGCA-3′ (reverse 5). Oligonucleotides containing siRNA target for *AIF* sequences were as follows: 5′-TGGAGGAGTCTGCGTAATGTTTCAAGAGAACATTACGCAGACTCCTCCTTTTTTC-3′ (forward 1) and 5′-TCGAGAAAAAAGGAGGAGTCTGCGTAATGTTCTCTTGAAACATTACGCAGACTCCTCCT-3′ (reverse 1); 5′-TGCAGGAAGGTAGAAACTGATTCAAGAGATCAGTTTCTACCTTCCTGCTTTTTTC-3′ (forward 2) and 5′-TCGAGAAAAAAGCAGGAAGGTAGAAACTGATCTCTTGAATCAGTTTCTACCTTCCTGCT-3′ (reverse 2); 5′-TGCATGCTTCTACGATATAATTCAAGAGATTATATCGTAGAAGCATGCTTTTTTC-3′ (forward 3) and 5′-TCGAGAAAAAAGCATGCTTCTACGATATAATCTCTTGAATTATATCGTAGAAGCATGCT-3′ (reverse 3); the nucleotide sequences corresponding to the siRNA are underlined. The resulting plasmids or the parental pLL3.7, along with lentiviral packaging mix (ViraPower, Invitrogen), was transfected into 293FT cells (Invitrogen) to produce recombinant lentivirus, and the UOC-B1 or UOC-B1/Survivin(dn) cells were infected with the virus. Enhanced green fluorescent protein (GFP)-positive cells were purified by FACSAria (BD Biosciences) as shRNA-transfected cell populations.

Reporter Assay—Fragments of the 5′-flanking region of the human *survivin* gene spanning 147, 213, 288, 503, or 698 bp were generated by PCR using *Pfu* polymerase from genomic DNA of human placenta. The positions of the forward (5′)

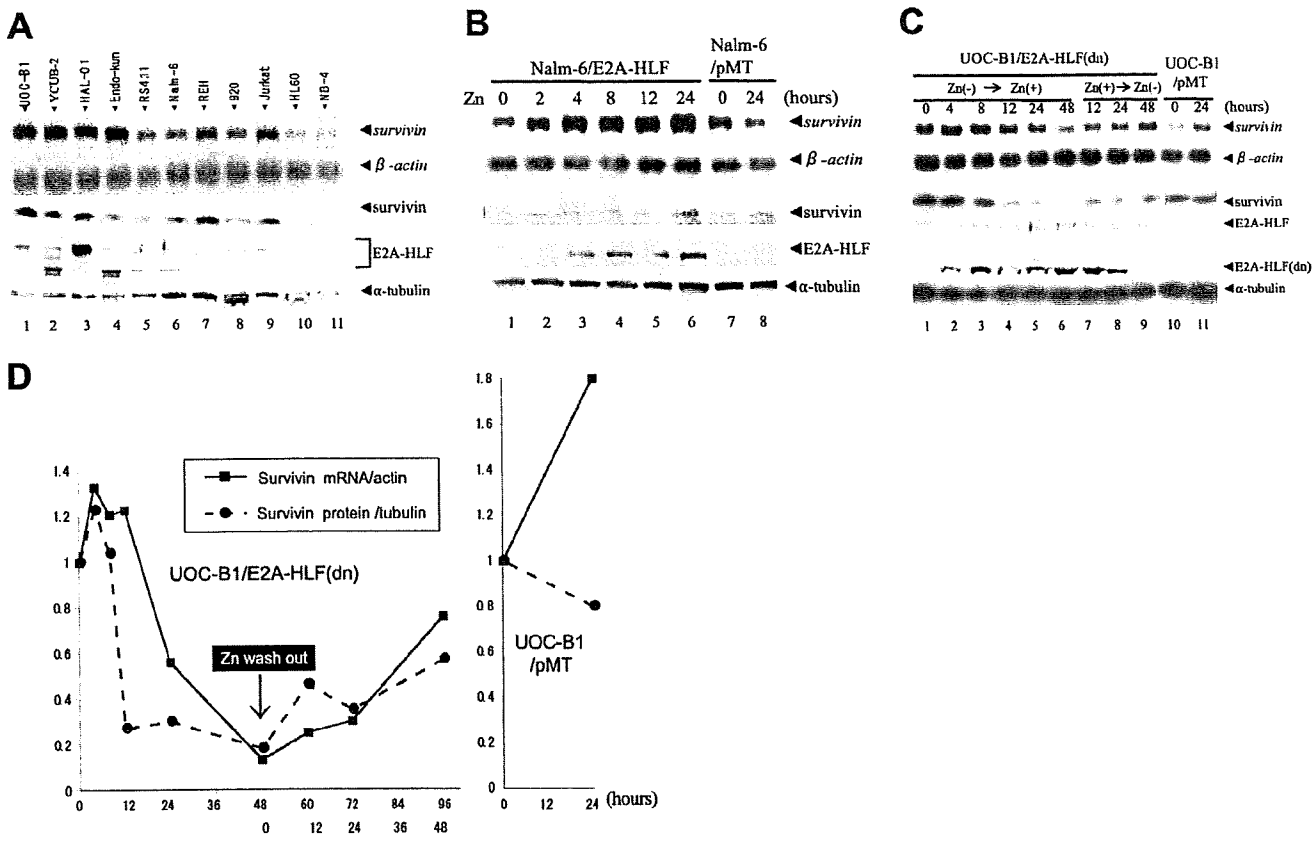

FIGURE 1. **Expression of Survivin in human leukemia cell lines and induction of Survivin by E2A-HLF in human ALL cells.** *A, top 2 panels,* Northern blot analysis of poly(A)$^+$ RNA isolated from human leukemia cell lines. The blot was hybridized with a *survivin* cDNA probe and then rehybridized with a β-actin probe. *Lower three panels,* immunoblot analysis using whole-cell lysates. Survivin, E2A-HLF, and α-tubulin proteins were detected with specific antibodies. *Lanes 1–4,* the UOC-B1, YCUB-2, HAL-01, and Endo-kun t(17;19)-positive pro-B ALL cell lines; *lanes 5–8,* the RS4;11, Nalm-6, REH, and 920 pro-B ALL cell lines without t(17;19); *lane 9,* the Jurkat T-ALL cell line; *lane 10,* the HL-60 AML cell line; and *lane 11,* the NB-4 APL cell line. *B,* Nalm-6 cells with zinc-inducible expression of E2A-HLF (Nalm-6/E2A-HLF) and control Nalm-6/pMT cells were cultured in medium containing 100 μM zinc for the indicated length of time. *C* and *D,* UOC-B1 cells with zinc-inducible expression of E2A-HLF(dn) (UOC-B1/E2A-HLF(dn)) and control UOC-B1/pMT cells were cultured in medium containing 100 μM zinc for the indicated length of time (*Zn*(−) → *Zn*(+)) and removal of zinc from the growth medium (*Zn*(+) → *Zn*(−)). *C, upper two panels,* Northern blot analysis of poly(A)$^+$ RNA. The blot was hybridized with a *survivin* cDNA probe and then rehybridized with a β-actin probe. *Lower three panels,* immunoblot analysis for Survivin, E2A-HLF, or α-tubulin proteins. *D,* quantification of intensity of each band.

primers with respect to the translational initiation codon (according to NCBI GenBank™ sequence U75285) are −124 (−124 forward primer, 5′-ACTCCCAGAAGGCCGCGGGGGGTG-3′), −190 (5′-ACCACGGGCAGAGCCACGCGGCGGG-3′), −265 (5′-GTTCTTTGAAAGCAGTCGAGGGGGC-3′), −480 (5′-CGGGTTGAAGCGATTCTCCTGCCT-3′), and −675 (5′-CGATGTCTGCACTCCATCCCTC-3′). The reverse (3′) primer used for these amplifications was at position 23 (+23-reverse primer, 5′-GGGGGCAACGTCGGGGCAagCtTGC-3′) and was constructed based on the genomic sequence with a modification (lowercase) to create a HindIII site. The PCR products were cloned into a pGL3-basic vector (Promega, Madison, WI). The resulting reporter plasmids were designated as pGL3-124, pGL3-190, pGL3-265, pGL3-480, and pGL3-675, respectively. The pGL3-124mut1 vector containing two mutated cell cycle-dependent elements (−6 and −12) was generated by PCR using the −124 forward primer and a reverse primer (5′-GCAAGCTTGtcactGtcactACCTCTG-3′); pGL3-124mut2 vector containing mutated CHR (−42) in addition to two mutated cell cycle-dependent elements (−6 and −12) was generated by the −124 forward primer and a reverse primer (5′-GCAAGCTTGtcactGtcactACCTCTGCCAACGGGTCCCGCGATTCgggTCTGG-3′); and pGL3-124mut3 vector containing a mutated CHR (−42) was generated by the −124 forward primer and a reverse primer (5′-GCAAGCTTGCCGCCGCCGCCACCTCTGCCAACGGGTCCCGCGATTCgggTCTGG-3′) (lowercase indicates mutations).

For transfection with a pMT-CB6$^-$/E2A-HLF construct, Nalm-6 cells (6×10^4) were seeded into 24-well plates, cotransfected with pGL3-*survivin* promoter construct plus pRL-TK vector, which contains the *Renilla* luciferase gene, by Lipofectamine 2000 (Invitrogen), and harvested 24 h later. E2A-HLF expression was induced in Nalm-6 cells by the addition of 100 μM $ZnCl_2$ 24 h after transfection. Firefly luciferase and *Renilla* luciferase as a transfection efficiency control were detected with Dual-Luciferase Reporter Assay System (Promega) according to the manufacturer's instructions and measured in a Veritas Microplate Luminometer (Promega).

Electrophoretic Mobility Shift Assays (EMSA)—EMSA were performed by incubating 12 μg of nuclear protein lysate at 30 °C for 15 min with a ^{32}P-end-labeled DNA oligonucleotide probe (2×10^4 cpm) containing the CHR-binding site sequence

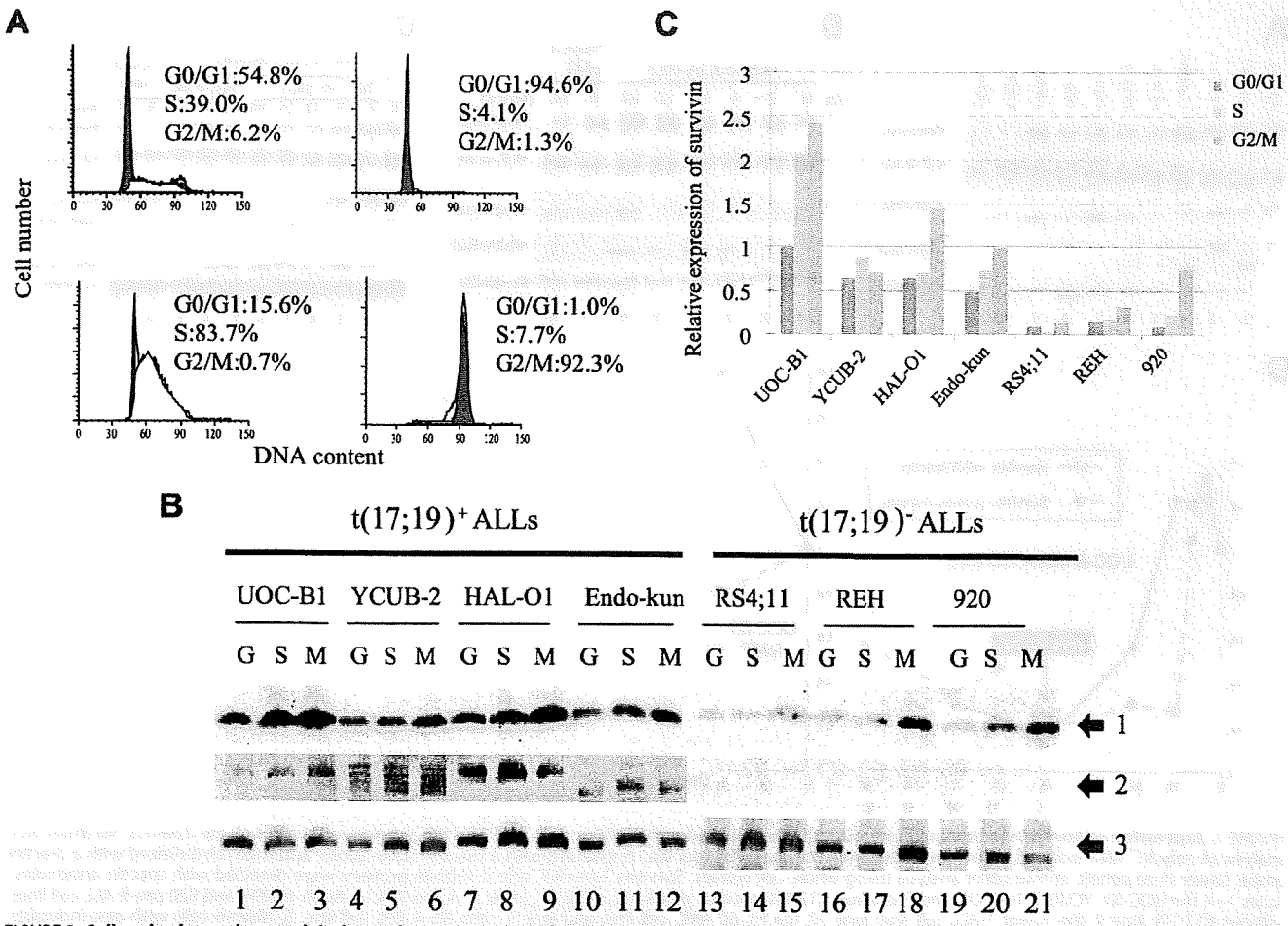

FIGURE 2. **Cell cycle-dependent and -independent expression of Survivin in human leukemia cells.** Fractions enriched with cells at each phase of the cell cycle were separated by counterflow centrifugal elutriation. *A*, representative DNA histogram of each fraction subjected to flow cytometry after staining DNA with PI. *Upper left*, no fractionation; *upper right*, G_0/G_1 phase-enriched fraction; *lower left*, S-phase-enriched fraction; *lower right*, G_2/M-phase-enriched fraction. *B*, immunoblot analysis of fractions of $t(17;19)^+$ ALL cells or $t(17;19)^-$ ALL cells enriched with cells in the G_0/G_1- (*G*), S- (*S*), or G_2/M (*M*)-phase. Survivin (*arrow 1*), E2A-HLF (*arrow 2*), and α-tubulin (*arrow 3*) proteins were detected with specific antibodies. *C*, levels of Survivin and α-tubulin proteins were determined by the band intensity on autoradiograms from *B*. Levels of Survivin were normalized to levels of α-tubulin, and amounts shown are relative to amounts in UOC-B1 cells in the G_0/G_1-phase.

in the *survivin* promoter (5′-CATTAACCGCCAGATTTGAATCGCGG-3′) in a solution of 12% glycerol, 12 mM HEPES (pH 7.9), 4 mM Tris (pH 7.9), 133 mM KCl, 1.5 μg of sheared calf thymus DNA, and 300 μg of bovine serum albumin per ml as described previously (24). In the competitive inhibition experiments, excess of the unlabeled CHR-consensus sequence probe, *i.e.* oligonucleotide containing the candidate-binding sites of CHR in the *survivin* gene promoter or its 3-bp mismatched oligonucleotide (5′-CATTAACCGCCAGAcccGAATCGCGG-3′) was added to the reaction mixture. The entire mixture was incubated at 30 °C for 15 min. Nondenaturing polyacrylamide gels containing 4% acrylamide and 2.5% glycerol were prerun at 4 °C in a high ionic strength Tris-glycine buffer for 30 min and run at 50 mA for ~45 min. The gel was then dried under vacuum and analyzed by autoradiography.

Other Experimental Procedures—For visualization of intracellular AIF, cytospinned cells were fixed with 1% paraformaldehyde in PBS for 10 min, and permeabilized with 0.5% Triton X-100 in PBS for 5 min. Cells were rinsed twice with PBS (5 min for each rinse), blocked with 5% goat serum in PBS for 30 min, and incubated with anti-AIF antibody (1:100; Santa Cruz Biotechnology, Santa Cruz, CA) overnight at 4 °C in a humidified chamber. Cells were incubated with a secondary antibody, fluorescein isothiocyanate (FITC)-labeled anti-goat IgG (1:500; Santa Cruz Biotechnology), at 37 °C for 30 min.

For Northern blot analysis, 1 μg of poly(A)-selected RNA was separated by electrophoresis in 1% agarose gels containing 2.2 M formaldehyde, transferred to nylon membranes, and hybridized with the appropriate probe according to standard procedures as described previously (5). For immunoblot analysis, the primary antibodies used were anti-Survivin polyclonal (R & D Systems, Minneapolis, MN), anti-α-tubulin monoclonal (Sigma), anti-caspase 3 polyclonal (Cell Signaling Technology, Beverly, MA), anti-caspase 9 polyclonal (BD Biosciences), anti-PARP monoclonal (BD Biosciences), and anti-AIF polyclonal antibodies (Santa Cruz Biotechnology). Anti-HLF(C) antibody for detection of the E2A-HLF chimeric protein was described previously (24).

Cell viability was determined by trypan blue dye exclusion. Early apoptotic events were detected by flow cytometric mea-

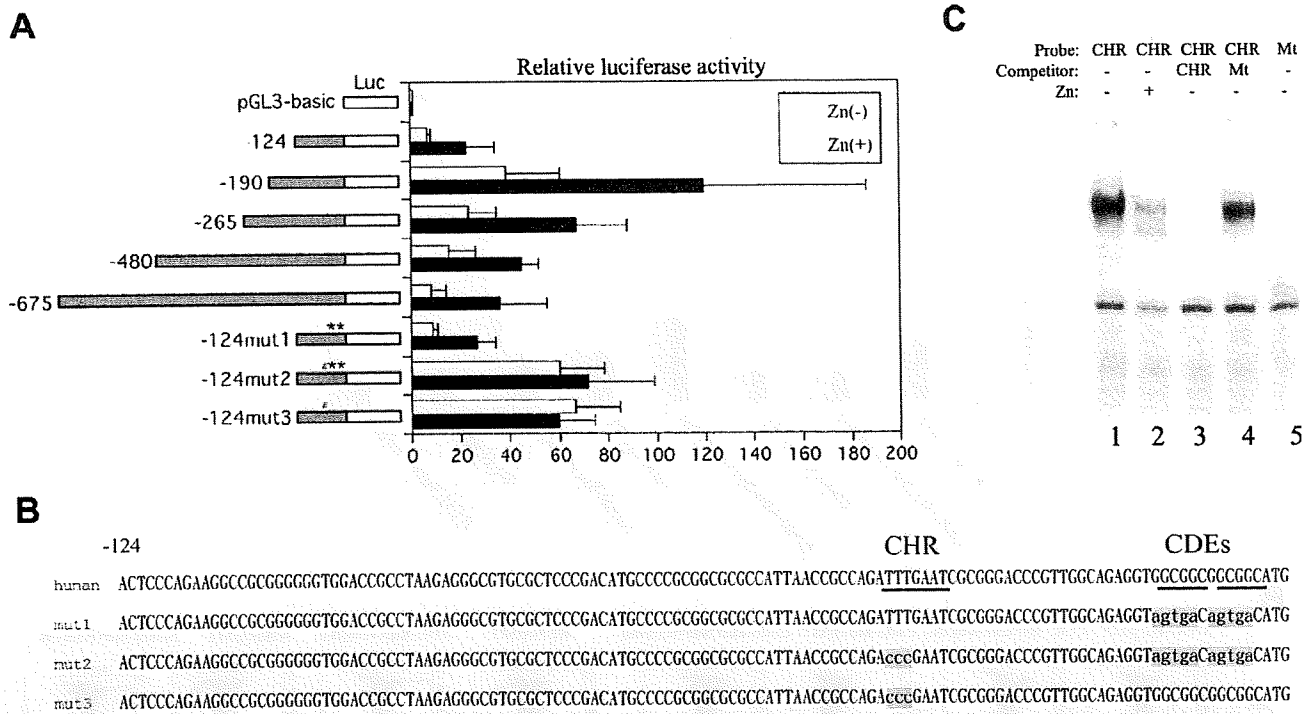

FIGURE 3. **Effect of E2A-HLF on *survivin* promoter activity in transiently transfected t(17;19)$^-$ ALL cells.** *A*, Nalm-6/E2A-HLF cells cotransfected with pRL-TK vector and the pGL3-*survivin* promoter constructs indicated at the *left* were cultured in the absence (*open bars*) or presence (*black bars*) of zinc for 24 h. Firefly luciferase (*Luc*) activity was normalized to *Renilla* luciferase as a transfection efficiency control. The level of activity of the promoterless *Renilla* plasmid luciferase was defined as 1. The results depicted are the averages of three independent experiments; *error bars* indicate S.D. # indicates mutation of CHR, and ** indicates mutation of CDE. *B*, nucleotide sequences of the human *survivin* promoter and three mutants. *Underlines* indicate CHR or CDE region. *Shaded characters* indicate mutation (*mut*). *C*, EMSA. Nuclear lysates extracted from Nalm-6/E2A-HLF cells cultured without (*lanes 1* and *3–5*) or with zinc (*lane 2*) were incubated with a ^{32}P-end-labeled oligonucleotide probe containing the CHR sequence (*lanes 1–4*) or mutated CHR sequence (*lane 5*). An excess of unlabeled CHR sequence competitor (*lane 3*) or mutant competitor (*lane 4*) was added to the reaction mixture. *Mt*, mutant.

surement of externalized phosphatidylserine with the annexin-V-FITC apoptosis detection kit I (BD Biosciences) in preparation for flow cytometry with the FACScan/CellFIT system (BD Biosciences). For caspase inhibition, 20 μM benzyloxycarbonyl-VAD-fluoromethyl ketone (BD Biosciences) was added to the cells 1 h before the addition of zinc. Terminal deoxynucleotidyltransferase-mediated dUTP nick-end-labeling (TUNEL) was performed using the apo-BrdUrd TUNEL assay kit (Molecular Probes, Eugene, OR). Briefly, cells fixed with paraformaldehyde and ethanol were incubated with BrdUrd and TdT for 1 h at 37 °C. BrdUrd uptakes were detected by Alexa dye-leveled anti-BrdUrd antibodies. Cells were stained by PI just before analysis using FACScan/CellFIT system.

RESULTS

E2A-HLF Regulates Survivin Expression—Cell lines were used in this study instead of primary patient samples, because t(17;19)$^+$ ALLs constitute only ~1% of childhood B-precursor ALLs (1–3). Four t(17;19)$^+$ ALL cell lines (UOC-B1, YCUB-2, HAL-O1, and Endo-kun) expressed the E2A-HLF chimeric protein on immunoblot analysis (Fig. 1*A*, *4th panel, lanes 1–4*) either as a slower (*lanes 1* and *3*) or a faster migration band (*lanes 2* and *4*) corresponding to difference in the fusion junction, as described previously (3). Of the seven t(17;19)$^-$ leukemia cell lines tested (RS4;11, Nalm-6, REH, 920, Jurkat, HL-60 and NB-4), none expressed the E2A-HLF chimera (Fig. 1*A*, *lanes 5–11*). We performed Northern blot and immunoblot analyses to test human leukemia cell lines for the expression of *survivin*. Survivin mRNA and protein were expressed at uniformly high levels in the four t(17;19)$^+$ ALL cell lines (Fig. 1*A*, *top* and *3rd panels*). By contrast, *survivin* mRNA levels varied among the t(17;19)$^-$ leukemia cell lines and appeared to determine Survivin protein expression levels in each line (Fig. 1*A*, *lanes 5–11*).

Next, we tested whether E2A-HLF induces the expression of Survivin. For these experiments, Nalm-6 cells were transfected with a pMT-CB6+/E2A-HLF construct to generate clones (Nalm-6/E2A-HLF) with zinc-inducible expression of E2A-HLF (Fig. 1*B*, *4th panel*). Ectopic expression of E2A-HLF in Nalm-6 cells induced *survivin* mRNA by 5-fold within 24 h after the addition of zinc (Fig. 1*B*, *top panel*). Accordingly, Survivin protein expression increased within 24 h after induction of E2A-HLF (Fig. 1*B*, *3rd panel*). In control Nalm-6/pMT cells, which contained the empty vector, Survivin expression was unaffected by zinc (Fig. 1*B*, *lanes 7* and *8*), confirming that the observed changes in Survivin expression were induced by E2A-HLF and not by zinc.

Induction of Survivin by E2A-HLF was further confirmed using UOC-B1/E2A-HLF(dn) cells, which express zinc-inducible E2A-HLF(dn), a dominant negative mutant of E2A-HLF (see under "Experimental Procedures") (6, 19). Survivin mRNA and protein expression in UOC-B1/E2A-HLF(dn) cells were high in the absence of zinc (Fig. 1*C*, *top* and *3rd panels, lane 1*; see also Fig. 1*D*) but decreased within 24 h after the addition of

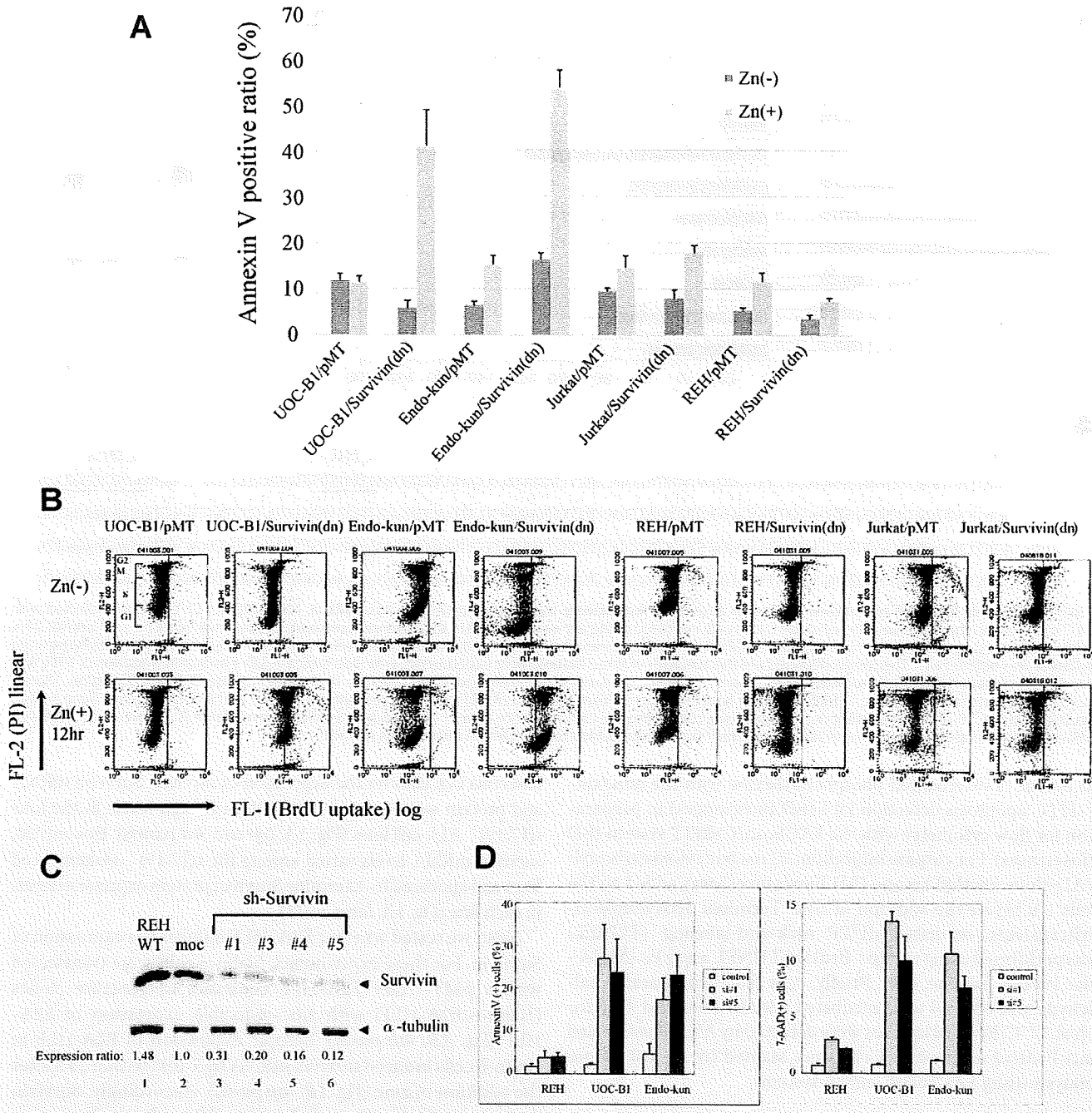

FIGURE 4. **Effect of enforced overexpression of Survivin-T34A and introduction of Survivin-shRNA in ALL cells.** UOC-B1, Endo-kun, Jurkat, and REH cells inducibly expressing Survivin-T34A (UOC-B1/Survivin(dn), Endo-kun/Survivin(dn), Jurkat/Survivin(dn) and REH/Survivin(dn) cells, respectively) were compared with control UOC-B1/pMT, Endo-kun/pMT, Jurkat/pMT, and REH/pMT cells, respectively. *A*, externalization of phosphatidylserine as determined by annexin-V binding. Cells cultured in medium with or without 100 μM zinc for 24 h were simultaneously stained with FITC-annexin-V and PI. The FITC-annexin-V-positive ratios were determined by representative flow cytometric plots. *B*, cells cultured in medium with or without 100 μM zinc for 12 h were simultaneously stained with PI and BrdUTP in a TdT-catalyzed reaction and then subjected to flow cytometric analysis. DNA ends labeled with BrdUTP (*abscissa*) are shown as a function of cellular DNA content of PI-stained nuclei (*ordinate*). Cells to the *right* of the *vertical line* had free DNA ends labeled with TdT, indicating apoptosis. Range of each cell cycle was shown in the panel of UOC-B1/pMT, *Zn*(−). *C*, immunoblot analyses using Survivin (*upper panel*) and α-tubulin (*lower panel*) antibodies. REH cells without treatment (*lane 1*) or infected with lentivirus (*lanes 2–6*) were sorted by GFP expression. *moc* indicates control sh-RNA. Ratios of intensity are shown *below*. *WT*, wild type. *D*, ratios of annexin-V-phycoerythrin (*PE*) (*left*) or 7-AAD (*right*)-positive cells in the GFP-positive fraction of REH, UOC-B1, or Endo-kun cells infected with lentivirus expressing GFP alone (control) or GFP and Survivin shRNA1 or -5 (*si#1* or *si#5*, respectively). Mean values from three independent experiments are shown with standard error.

zinc (Fig. 1*C*, *lane 5*), coincident with expression of E2A-HLF(dn) protein (*4th panel*). Removal of zinc from the growth medium restored Survivin expression within 48 h, again coincident with a decline in the E2A-HLF(dn) protein level (Fig. 1*C*, *lane 9*). These data suggested that E2A-HLF induces Survivin mRNA expression. Down-regulation of Survivin protein pre-